Department of Chemical Engineering

Faculty of Engineering and the Built Environment

University of Cape Town

Study of Selective Removal of CoS and NiS during Purification of $MnSO_4$ Electrolyte

Vuyiswa Dube

Prof. Alison Lewis and Dr Marcos Rodriguez Pascual

2015

Submitted in fulfilment of the requirements for the degree of

Master of Science in Engineering

Declaration

Plagiarism Declaration:

I know that plagiarism is wrong. Plagiarism is to use another's work and pretend that it is my own. I have used the Harvard system for citation and referencing. In this report, all contributions to, and quotations from, the work(s) of other people have been cited and referenced. This report is my own work. I have not allowed, and will not allow, anyone to copy my work

……..

Signed: Vuyiswa Dube

Acknowledgements

I would like to thank God the Almighty for his guidance and grace for helping me through this journey.

I express my sincere gratitude to my supervisor, Prof. Alison Lewis for offering me the opportunity to be part of this field of research. I thank Dr. Marcos Rodriguez Pascual for the continuous support, for his patience, motivation and enthusiasm. His guidance helped me throughout this research and writing of this thesis.

To my fellow CPU group mates, Lucia Dzinza, Emily Mayer de Andrade Becheleni, Sibongiseni Gqebe, Dereck Ndoro, Edward Peters, Jemitias Chivavava, Michael Kapembwa and Moses Nduna thank you for the insightful comments, stimulating discussions, and for all the fun we have had in the last two years.

Engineer Gordon Lister from Kromboom Rotary International Club, l am glad you took some time to proof read this work. Thank you for the invaluable input to this research project.

To my family: my mother Ntombiyejele Ncube, my husband, Nqobizitha Ncube, my daughter Aderline Ncube and my siblings Sanelisiwe and Ayanda Dube thank you for the inspiration, support and encouragement. You are the best.

I am very grateful to the South African Water Research Commission for sponsoring and funding this research study done under the auspices of the Crystallization and Precipitation Research Unit.

Abstract

This research project investigated the selective removal of Co^{2+} and Ni^{2+} from a Co-Ni-Mn system through sulphide precipitation. The Co^{2+} and Ni^{2+} ions have adverse effects on the purity of the manganese product, thus, have to be removed via precipitation in a purification step. The main objective of this research was to understand the influence of local supersaturation on the purification process. This was important for controlling such a process to achieve residual ion concentrations of 0.3 ppm and 1.0 ppm for Co^{2+} and Ni^{2+} ions respectively, with minimum loss of the Mn^{2+} ions.

Preliminary work evaluated the effect of mixing on selective removal of these metal impurities. This was achieved by comparing a semi batch stirred tank reactor (STR) with a double jet parallel reactant addition method and a T-premixed reactor (TPR). The residual concentrations of Ni^{2+}, Co^{2+} and Mn^{2+} were measured using ICP-OES and particle characterisation was obtained using a Malvern Mastersizer 2000, X-Ray Diffraction (XRD) and Scanning Electron Microscopy (SEM). It was found that at low supersaturation levels, removal of impurities was the same in both mixing configurations. However at high supersaturations, the TPR configuration achieved greater removal of Co^{2+} and Ni^{2+} from a system of Co-Ni-Mn. Additionally, the resulting particles had a much larger average modal particle size of about 32 μm.

The TPR was then adopted for investigating the effects of operating conditions on removal of these impurities. The two main variables were pH and batch residence time. Experiments were conducted under inert conditions, at a constant temperature of 35^0C, using a synthetic solution with a typical industrial composition of 10 mgL^{-1} Co^{2+}, 100 mgL^{-1} Ni^{2+} and 32 gL^{-1} Mn^{2+}. This was reacted with ammonium sulphide of equi-molar concentration to that of both the metal impurities. The pH levels investigated were 4.8, 6.5, 7.0 and 7.8. Collected samples were analysed for residual concentrations of Ni^{2+}, Co^{2+} and Mn^{2+} using ICP-OES, in order to determine the precipitated amounts. The mechanism of co-precipitation of MnS was determined by analysing residual ion concentrations, at a pH level of 7.0 for batch residence times of 10 mins, 30 mins and 45 mins.

A comparison of the thermodynamic equilibrium concentration of metal sulphides to those obtained experimentally indicated no significant influence of pH on the extent of impurity removal. The maximum CoS removed was only 49.2% and that of NiS was 86.6%, at pH 7.8. However, the co-precipitation with Mn^{2+} significantly increased within pH levels of 4.8-6.5.

A maximum loss of 9.12% of Mn^{2+} was obtained. It was further demonstrated that at a pH level of 7.0 and batch residence times of 10, 30 and 45 minutes, this co-precipitation was temporal, the concentration of Mn^{2+} ions increased with an increase in batch residence time. The extent of this mechanism was limited by the batch times investigated.

Table of Contents

Table of Contents

Table of Contents

List of Figures

List of Tables

Nomenclature

ABBREVIATION LIST

ICP-OES	Induced Coupled Plasma Optical Emission Spectrometry
IAP	Ionic Activity Product
MSMPR	Mixed Solid, Mixed Product Removal Reactors
PSD	Particle Size Distribution
SEM	Scanning Electron Microscopy
STR	Stirred Tank Reactor
TPR	T-Premixed Reactor
XRD	X-Ray Diffraction

GREEK SYMBOLS

ρ	Density (kg/m^3)
σ	surface area (m^2)
γ	Interfacial energy (J)
η	Viscosity (Pa/s)
μ	Chemical potential (J/mol)
μ^*	Chemical potential at equilibrium (J/mol)
ε	Energy dissipation rate
Λ	Macro scale turbulence (m)

Nomenclature

a	Activity (mol/dm^3)
a^*	Activity at equilibrium (mol/dm^3)
C	Concentration (mol/dm^3)
C^*	Equilibrium concentration (mol/dm^3)
C_b	Bulk concentration (mol/dm^3)
C_i	Concentration at solution interface (mol/dm^3)
D	Diameter (m)
D_{meso}	Turbulent diffusivity (m^2/s)
f	Darcy friction factor
G	Gibbs energy (J)
g	Gravity (m/s^2)
k	Boltzmann's constant (J/molecule.K)
k_d	Mass transfer coefficient
k_r	Reaction rate constant
K_{sp}	Solubility product
N	Impeller speed (rps)
Nq	Flow number
Q	Volumetric flow rate (m^3/s)
q_c	Pumping capacity (m^3/s)
P	Power (W)
R	Universal gas constant (J/mol.K)
S	Supersaturation ratio
T	Temperature (kelvin)
t_{macro}	Macro - mixing time (s)
t_{meso}	Meso - mixing time (s)
t_{micro}	Micro - mixing time (s)
t_c	Circulating time (s)
u	Fluid velocity (m/s)
V	Volume of reactor (m^3)

1 INTRODUCTION

1.1 Background

The purification of hydrometallurgical streams is usually practised in most mining extraction processes to remove metal impurities prior to recovery of valuable mineral. In the manganese ore refining process, the sulphuric acid used in the leaching stage is rarely, if ever completely selective. The resulting aqueous manganese (II) sulphate electrolyte contains very small amounts of metal impurities such as iron, zinc, cobalt and nickel ions, compared to that of the valuable manganese metal ions. Of these metal impurities, cobalt has an adverse effect on the electric current efficiency in the subsequent electro winning stage and thus compromises the purity of the final manganese product (Bryson & Bijsterveld, 1991).

According to Harris and co-workers (1977), the maximum levels of impurities that can be tolerated in the cell feed of the electro-winning cell should be less than 1ppm and 0.3ppm for Ni^{2+} and Co^{2+} ions respectively. The presence of these impurities is practically evidenced by the re-dissolution of deposited manganese product and by formation of black borders around the deposition area. In some cases, very brittle, pin holed nodular deposits are formed which are difficult to remove from the cathode. Complete flaking of deposited manganese solids is also observed on the cathode electrodes (Harris, Meyer & Auerswald, 1977).

Precipitation of these metal impurities using ammonium sulphide, through a sulphide precipitation technique has been commercially accepted for the purification of manganese (II) electrolyte streams (Wanamaker & Morgan, 1943; Jacobs, 1946; Bryson & Bijsterveld, 1991). There are several advantages that have made this technique a preferred choice to purify and recover metals from multi-metal ionic streams. These include feasibility for selective sequential separation due to differences in metal sulphide solubility products, over a broad pH range (Bryson & Bijsterveld, 1991; Mishra & Das, 1992; Veeken & Rulkens, 2003; McGeorge, Gaylard & Lewis, 2009), fast reaction kinetics (Rickard, 1989), high degree of metal removal (Peters, Young & Bhattacharyya, 1985) to low residual concentrations below 0.00001 mg/L (Lewis, 2010) and formation of relatively low sludge volumes (Bhagat et al., 2004) of good solid-liquid settling properties.

However, sulphide precipitation is not widely practiced due to poor control of sulphide dosing and handling concerns posed by toxicity and corrosiveness of excess sulphide (Veeken & Rulkens, 2003). Alternative precipitation processes use biogenic sulphide (Bhagat et al., 2004; Sahinkaya E. et al., 2009; Reis et al., 2013) as this can be produced on demand at site and has significant cost savings. There is also the additional benefit of improved safety due to the elimination of the transportation, handling and storage required for chemical sulphide reagents.

Selectivity of metal impurities during purification depends significantly on their metal sulphides' solubility products and control of supersaturation (Jandová et al., 2005). This is directly affected by mixing, concentration of sulphide ions and precision in the pH value at which precipitation takes place (Veeken & Rulkens, 2003; Sampaio et al., 2009; Villa-Gomez et al., 2012).

The selective removal of impurities from a manganese (II) sulphate electrolyte is usually compromised by the fact that the operating pH required to achieve the desired residual concentrations of impurities also promote co-precipitation with manganese ions. In order to address this challenge, an understanding of the influence of local supersaturation on the selective removal of impurities has to be exploited, to explain the necessity of co-precipitation of valuable metal ions. This is important for process design and optimisation of purification systems.

1.2 Scope of Research

For precipitation purification processes, the operating conditions, the quality of the bulk concentrate stream (for example, residual impurity concentration) and the properties of the precipitate (for example, chemical composition, co-precipitation, particle size distribution (PSD), morphology and density) are important aspects of controlling this process (Ntuli & Lewis, 2009).

Thus, this research study was limited to the effects of pH on selective removal of metal impurities as sulphides from a Co-Ni-Mn stream, using either a semi batch stirred tank reactor (STR) or a T-premixed reactor (TPR). The choice of the best mixing configuration

was based on a comparison of selectivity, PSD and morphology based on the SEM images. The multi-metal ionic electrolyte used was typical of industrial compositions, rich in manganese ion concentration and orders of magnitudes lower in Co^{2+} and Ni^{2+} ion concentrations. This stream comprised of 32 g/L Mn^{2+}, 100 mg/L Ni^{2+} and 10 mg/L Co^{2+}. The pH levels tested were obtained from a thermodynamic model. These were limited to those that significantly favour minimal Mn^{2+} ion co-precipitation and promote high removal degree for Co^{2+} and Ni^{2+} ions to levels below 1 ppm. The operating temperature was kept constant at 35 ^{0}C for all experimental investigations. However, it is appreciated that other factors may affect the purification process of this stream such as sulphide ion concentration, temperature, pressure, and precipitate recycle.

1.3 Structure of Dissertation

This dissertation is structured into six chapters. Chapter 2 gives a detailed introduction to precipitation theory that includes supersaturation and kinetic processes. A comprehensive literature review in Chapter 3 summarises the findings and discussions in the field related to selective removal of impurities, factors affecting this purification and the kinetics studies during purification of hydrometallurgical streams. Chapter 4 gives a detailed description of the thermodynamic model used, apparatus, experimental procedures and the analytical techniques used in the study. The obtained results and associated discussions are in Chapter 5. The conclusions and recommendations from this research are stated in Chapter 6. The appendices include raw data, sample calculations and the faculty ethics form.

2 THEORY

An introduction to important aspects of metal sulphide precipitation theory is described in this chapter. The definition and concept of supersaturation and solubility on precipitation is given. The kinetic processes of nucleation, growth, agglomeration and aggregation are also highlighted. A brief description of the mixing and mixing scales commonly associated with these precipitation processes concludes this section.

2.1 Introduction to precipitation

Sohnel and Garside (1992) refer to precipitation as a relatively fast crystallisation process characterised by the formation of a sparingly soluble solid phase of solubility in the range of 0.001-1 kg/cm^{-3}. The high supersaturation and rapid kinetics render precipitation processes susceptible to primary nucleation over growth. This results in formation of a large number of particles typically within the ranges of 10^{11} -10^{16} particles per cm^3, with relatively small particle size ranges of 0.10 -10 μm (Sohnel & Garside, 1992). The quality of the shapes of the precipitated particles is very poor hence, are usually amorphous and polymorphs. This is also governed by the extent of secondary processes such as agglomeration, aggregation, Ostwald ripening and ageing.

Precipitation is employed in hydrometallurgical systems for the potential of formation of solids with specified particulate properties usually of high yield and /or efficiency in metal separation and high degree of removal of metal impurities and minor metal constituents (Jackson, 1986). Precipitation is largely used to recover dissolved valuable metal ions from industrial waste water prior to discharge. The technique is also fast gaining popularity in micro-nano particle technology.

2.2 Supersaturation

Supersaturation rules the thermodynamic driving force behind all precipitation processes. Equation 1.0 represents a typical reaction of precipitation of a solid from dissolved ionic species.

$$xA^{z+} + yB^{z-} \leftrightarrow A_xB_y \quad 1.0$$

Considering this equation, Mersmann (2001) described supersaturation as the difference, Δμ, between the chemical potential of the solute in solution, μ, and the chemical potential of the solution in equilibrium with the solid phase, μ^*, as defined by the Equation 1.1.

$$\Delta\mu = RT \ln(\frac{a}{a*}) \quad 1.1$$

Where a is the activity of the reacting species in solution and a^* is the activity of the reacting species at equilibrium. This equilibrium activity is described by as the solubility product (K_{sp}) which is commonly expressed by Equation 1.2. Thus, for metal sulphide precipitation from dissolved ionic species.

$$K_{sp} = a^*_{Me^{2+}}.a^*_{S^{2-}} \quad 1.2$$

Supersaturation can also be expressed as the product of the activities of the reacting species to the solubility product as described in Equation 1.3 (Sohnel & Garside, 1992; Mersmann, 2001).

$$S = \left(\frac{(a_{Me^{2+}})^1\left(a_{S^{2-}}\right)^1}{K_{sp}}\right)^{\frac{1}{2}} \quad 1.3$$

Accordingly, saturation ratio, *S*, in aqueous solutions of sparingly soluble electrolytes may be expressed in terms of the ionic activity product (IAP), of the lattice ions in solution, the solubility product (K_{sp}) and the number of ions in a formula unit of the salt (v), as indicated in Equation 1.4 (Mullin, 2001). This relationship makes it possible to predict whether the sparingly soluble salt will dissolve or precipitate.

$$S = \left(\frac{\text{IAP}}{K_{sp}}\right)^{\frac{1}{v}} \quad 1.4$$

The saturation ratio, *S,* is determined from relations with the saturation indices (SI), that are easily obtained from thermodynamic models. Equation 1.5 and 1.6 summarises this relation.

$$SI = \log (IAP) - \log K_{sp} \quad 1.5$$

$$\log S^2 = \log (IAP) - \log K_{sp} \quad 1.6$$

At saturation, SI is equal to zero. A value close to zero could indicate that the concentrations of reacting species are controlled by the presence of sparingly soluble salt. A negative SI means that the solution is undersaturated with respect to the metal salt (IAP < *Ksp*). Any metal salt present in the solid phase is thermodynamically unstable and could be expected to dissolve. If SI is greater than zero, the solution is oversaturated and precipitation of metal salt is favoured. In the same way, if *S* value is below zero the system is undersaturated, if S is equal to 1 the system is saturated and if S > 1 then the system is oversaturated.

2.2.1 Solubility of Metal Sulphides

The amount of solute required to make a saturated solution at a given condition of pH, temperature, pressure and concentration is defined as solubility of a particular substance (Myerson, 2002). When this solute concentration in the solvent exceeds its solubility the solution becomes supersaturated. Precipitation only occurs when a solution is supersaturated. This supersaturation may be created when a very insoluble product is formed from a reaction between two or more soluble reactants.

Figure 1 is an equilibrium solubility diagram which illustrates the relationship between solubility and different regions of saturation. Precipitation does not occur in the regions marked under-saturated as the particles formed in this usually dissolve. Although, the metastable region is a supersaturated region, spontaneous crystallization is highly unlikely (Mullin, 2001), nucleation and particle growth may only be promoted through seeding. A number of factors determine the width of this metastable region. These include the degree of agitation, concentration of crystalline solids and solutes that are present in solution. Spontaneous nucleation is only probable, but not inevitable in the labile region.

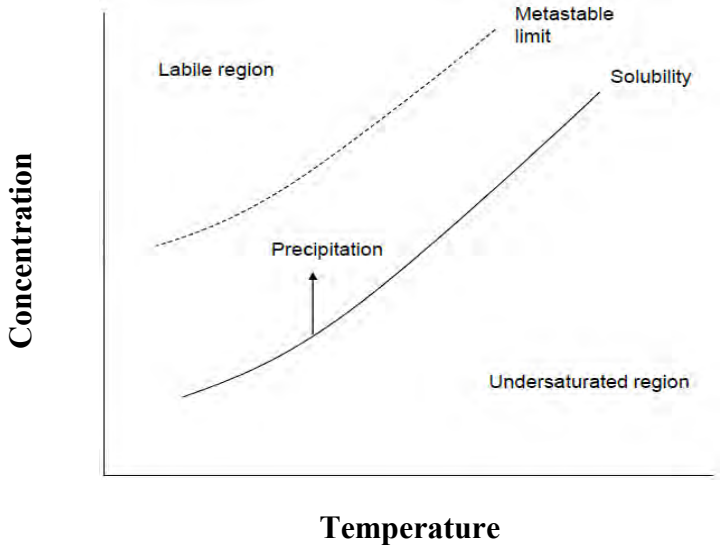

Figure 1: Relationship between supersaturation and solubility

Solubilities of metal sulphides are usually represented as solubility products from which the concentration of individual reacting ionic species in a saturated solution can be determined.

Table 1 provides the typical solubility products for various metal sulphides at room temperature. The low K_{sp} suggests that precipitation forms sparingly soluble solids and even at low reagent concentrations, the level of supersaturation remains high. Ideally, copper sulphide being the least soluble, precipitates out first, followed by zinc sulphide, cobalt sulphide, nickel sulphides, iron sulphide then finally manganese sulphide.

Table 1: Solubility Products for Metal sulphides at 25^0C (Jackson, 1986)

Metal sulphides	**Formula**	**Solubility Product**
Manganese sulphide	MnS	$3.16x10^{-11}$
Iron (II) sulphide	FeS	$7.94x10^{-19}$
Nickel sulphide	NiS	$3.98x10^{-20}$
Cobalt sulphide	CoS	$3.98x\ 10^{-22}$
Zinc sulphide	ZnS	$2.00x10^{-25}$
Copper (II) sulphide	CuS	$7.94x10^{-37}$

2.3 Kinetic Processes

Precipitation of soluble and sparingly soluble solids occurs by a number of kinetic processes. The reactants mix to form the first stable precipitated nuclei through a nucleation process. These grow under supersaturated condition, the particle characteristics and purity of the residual solution is governed by secondary processes of aggregation and agglomeration.

2.3.1 Nucleation

Nucleation is commonly defined as the formation of the first thermodynamically stable solid from a supersaturated solution (Sohnel & Garside, 1992). Nucleation occurs through two main mechanisms namely primary and secondary nucleation as shown in Figure 2.

Primary nucleation is the spontaneously new phase formation from clear solution. This can be subdivided into homogenous and heterogeneous nucleation. Homogenous nucleation describes new phase formation by statistical fluctuations of solute entities clustering together and heterogeneous is by presence of tiny foreign substrates. Secondary nucleation on the contrary, is induced at the interface of parent crystals at low to moderate supersaturations. The different types of secondary nucleation are named after their origin such as, initial/dust; dendritic, attrition and fluid shear breeding's. The creation of small nuclei requires extra free energy associated with the interfacial energy and the creation of surface (Lewis et al., 2012).

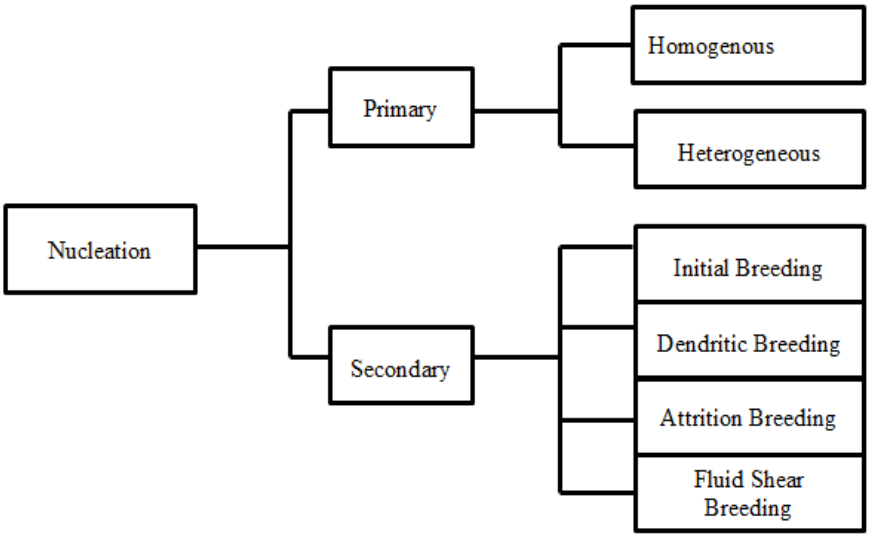

Figure 2: Nucleation Mechanisms (Lewis et al., 2012)

The relationship of the interfacial energy, γ, between the nucleating phase, surface area created by clusters, σ(i), and the solution is given in Equation 1.7. The symbol, ΔG(i), represents the work of formation of a mole of clusters consisting of i molecules from a solution at supersaturation S.

$$\Delta G(i) = -iRT\ln(S) + \gamma.\sigma(i) \qquad 1.7$$

2.3.2 Growth

Crystal growth is when the thermodynamically stable nuclei grows into larger particles by deposition of solute from the supersaturated solution (Myerson, 2002). The shape, surface structure and purity of the crystals are determined by the growth rate and mechanism.

Figure 3 illustrates the growth mechanism of the surface of a growing crystal. Firstly, the growth units of molecules, ions, clusters or monomers, are transported from the bulk solution to the solution-crystal interface by bulk diffusion. These are then incorporated into the crystal lattice through surface integration. The mechanism of crystal growth involves several steps which can be summarised as follows:

a) Transport of ions from the bulk solution to the solution immediately adjacent to the crystal surface,
b) Transfer of ions from the solution to an adsorption layer,
c) Transfer of ions from the solution or adsorption layer to a growth step,
d) Transfer of ions from the solution, adsorption layer or growth step to a growth site, for example, a lattice position at a kink.

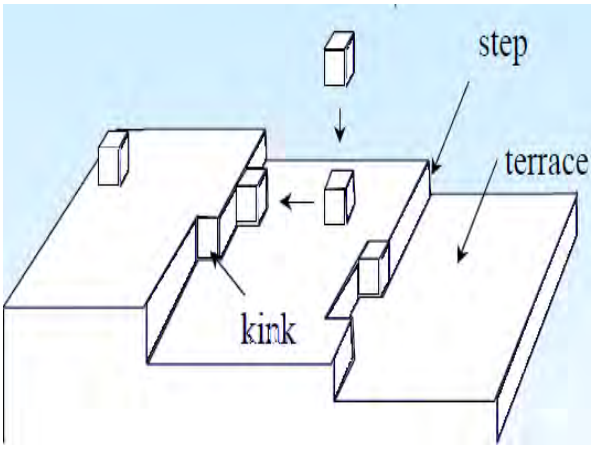

Figure 3: Diffusion and integration of growth units into crystal surface (Lewis et al., 2012)

Figure 4 illustrates the concentration profile perpendicular to the crystal surface during diffusion and integration. Where C_b is the bulk concentration, C_i, the concentration at the crystal solution interface and C^*, the equilibrium is the concentration at the growth site. Growth rate for highly soluble compounds is defined by the diffusion through the stagnant film or diffusion layer with thickness, sigma at the interface. The driving force for this process is given by C_b-C_i. However, for poorly soluble compounds, the rate limiting step is surface integration and the associated driving force is given by C_i-C^*.

Growth rate for a diffusion limited process may also be expressed as in Equation 1.8 and 1.9. Where, *i* represents conditions at the interface, * represents conditions at equilibrium, k_d is the diffusion mass transfer coefficient, k_r is the reaction rate constant for surface integration, *r* is the order of integration and *C* is concentration. Temperature dependence of the reaction rate constant is generally defined by the Arrhenius equation (Mullin, 2001).

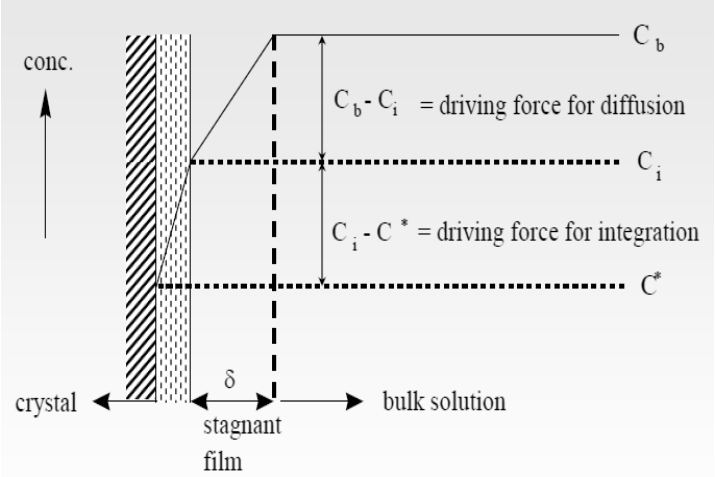

Figure 4: Concentration during crystal growth (Mullin, 2001)

$$G = k_d(C - C_i) \quad 1.8$$

$$G = k_r(C_I - C^*) \quad 1.9$$

Moreover, Mullin (2001) describes the mechanisms of surface integration growth to be greatly influenced by the levels of supersaturation. At low supersaturation, growth tends to be smooth and spiral, the 'birth and spread' models apply. The two dimensional nucleation

processes are promoted at moderate supersaturation levels whereas linear rough surface growth dominates at higher levels. This is summarized in Figure 5.

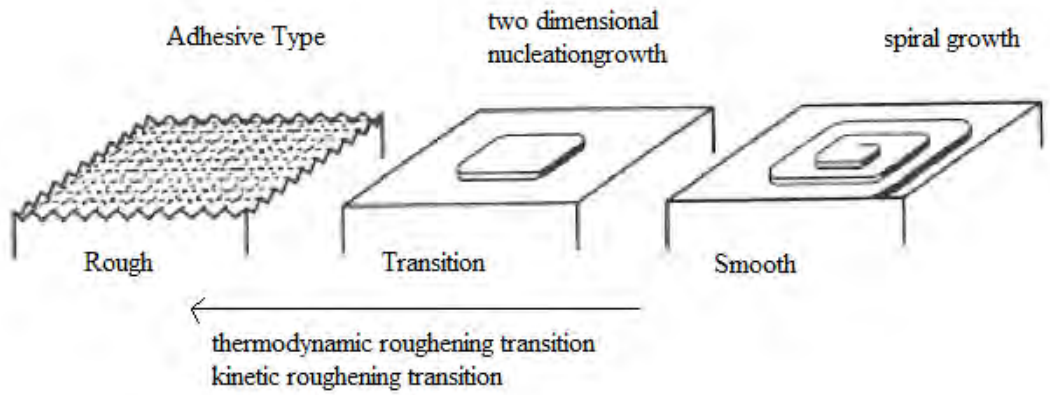

Figure 5: Effect of supersaturation on crystal growth mechanisms (Lewis et al., 2012)

Figure 6 illustrates the dynamic relationship between supersaturation and these kinetic processes of precipitation. Generally, at low supersaturation levels, growth rate dominates nucleation processes and consequently, the particle size is relatively large. Increasing the supersaturation promotes nucleation rate and produces very fine particles. This also results in a significant agglomeration rate promoting an increase in particle size due to agglomeration and aggregation.

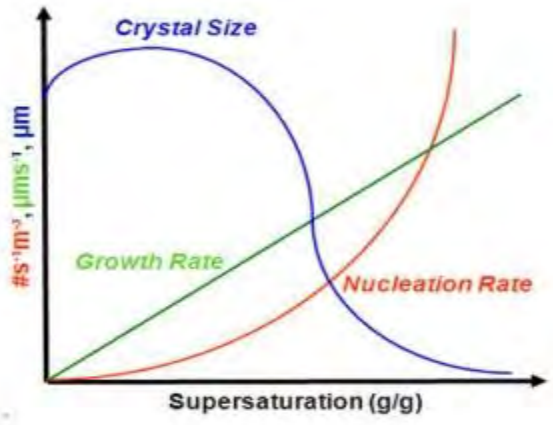

Figure 6: Relationship between supersaturation and kinetic rate processes (O' Grady, 2011).

2.3.3 Aggregation

This is defined as a process by which particles collide and adhere to be eventually cemented together to form stable particles (Sohnel & Garside, 1992). The theoretical mechanism of aggregation involves a number of steps including collision of particles, particle-particle interaction, repulsion and cementation.
The following is a detailed summary of the aggregation mechanisms:

1. The collision of particles

Particles collide through Brownian motion and/or diffusion also referred to as peri-kinetic aggregation. Ortho-kinetic aggregation is the collision due to hydrodynamic motions, such as convective currents and mechanical stirring. The most common type of collision of particles is inertial collision where particles settle due to the influence of a gravitational field.

2. Particle –particle interaction

Particles are attracted to one another through weak Van der Waals forces. These become weaker with separation distance. The collision efficiency and disruption of these aggregates, is also governed by the degree of repulsive and attractive interactions when particles come together. The shape and orientation of particles may dictate the collision efficiency of particles.

3. Cementation of the particles by growth to form agglomerates

2.3.4 Agglomeration

Agglomeration is defined as the phenomena in which particles are loosely bound together (Randolph & Larson, 1988), and involves the cementing together of particles by the formation of inter-particle crystalline bridges. This is a reversible process with the rate of aggregation and break-up being dependent on the control of a number of parameters such as mixing, supersaturation, solids concentration, pH and ionic strength (Grulietti et al., 2001).

2.4 Mixing in Precipitation Processes

2.4.1 Macro-mixing

This is the bulk dispersion of a liquid throughout reaction volume. it has been developed that for a well baffled tank, and fully developed turbulence, the macro-mixing time, t_{macro} [s],is between three to five times the circulating time, t_c[s],yielding:

$$t_{macro} = 4\, t_c \qquad 2.0$$

For a vessel with an impeller and four pitched blades, the circulation time is expressed as:

$$t_c = \frac{V}{q_c} \qquad 2.1$$

Where V,is the volume of the reactor [m^3] and q_c is the pumping capacity of the impeller [$m^3.s^{-1}$],which can be expressed as:

$$t_c = NqND^3_{stir} \qquad 2.2$$

Where N_q= flow number (taken as 0.73 for a pitched blade turbine)

N= impeller speed (rps)

D=impeller diameter (m)

Macro-mixing is ideal for residence times greater than 10s.

2.4.2 Meso-mixing

This is the convective exchange of fluids at the reactor inlets and occurs at a scale comparable to the size of the reagent feed pipe.

Two meso-mixing mechanisms have been identified:

- Inertial-convective disintegration of large eddies in the course of dispersion.
- Turbulent dispersion in the, feed stream spreads out transverse to its local streamline.

$$t_{\text{meso}} = \frac{Q}{uD_{\text{meso}}} \quad 2.3$$

Where Q=volumetric reactant flow rate [$m^3.s^{-1}$], u is the feed flow velocity [$m.s^{-1}$], and D_{meso} is the turbulent diffusivity [m^2s^{-1}].

The time constant for meso-mixing due to inertial convective disintegration of large eddies, is determined from (Torbacke & Rasmuson, 2001).

$$t_{\text{meso}} = a.\sqrt[3]{\left(\frac{\Lambda^2}{\varepsilon}\right)} \quad 2.4$$

Where a = 1-2 (2 for fully developed turbulence)

Λ = macroscale turbulence [m]

ε = local energy dissipation rate

(Torbacke & Rasmuson, 2001) also estimated the macro scale turbulence as:

$$\Lambda = \frac{\sqrt{Q}_{\text{b}}}{\pi u} \quad 2.5$$

Where Q_b= reactant flow rate [m^3/s]

u=fluid velocity [m/s]

The local dispersion rate is also estimated as:

$$\varepsilon = \frac{N_{\text{p}}N^3D^5}{V} \quad 2.6$$

Where N_p=power number (taken as 1.5 for pitched blade).

$$\text{N}_{\text{p}} = \frac{Pg}{\rho N^3D^5} \quad 2.7$$

Where P = power [W], g =acceleration by gravity [$9.81ms^{-2}$] and ρ = liquid density [kgm^{-3}]

The time constant for meso-mixing, due to turbulent dispersion is determined by the Equation 2.8.

$$\text{t}_{\text{d}} = \frac{Q_{\text{f}}}{uD} \quad 2.8$$

In either macro-mixing or meso-mixing, of slow to medium residence times scales, the concentration of metal ions is monitored by in-situ- optical absorption, polarimetry, ion-selective electrodes and conductivity. The sample is collected at intervals and the reaction is quenched. Quenching is done through freezing and neutralization techniques.

2.4.3 Micro-mixing

This is homogenization on the molecular scale through diffusion, laminar deformation of striations below the Kolmogorov scale and by mutual engulfment of regions having different compositions. This directly influences the chemical reaction, nucleation and crystal growth,(Myerson, 2002). The micro-mixing time is expressed from the local specific energy dissipation rate, (Baldga & Bourne, 1989).

$$t_{micro} = 17.24\left(\frac{\nu}{\varepsilon}\right)^{0.5} \quad 2.9$$

Where ν is the kinematic viscosity and ε , is the average energy dissipation rate estimated in Equation 3.0 as:

$$\varepsilon = \frac{Q\Delta P}{\rho V} = \frac{2fU^3}{D} \quad 3.0$$

Q is the flow rate, V, volume of outlet tube and f, Darcy friction factor for the tube walls, U, average flow velocity, D, internal diameter of tubing, ρ, density of fluid and ΔP, is the pressure drop.

The Blasius Equation 3.1 is the most simple equation for solving the Darcy friction factor for smooth pipes. It is valid for up to the Reynolds number of 10^5.

$$f = 0.316\ \mathrm{Re}^{-0.25} \quad 3.1$$

Flow experiments are common for study of reactions of fast kinetics where micro-mixing and diffusion dominates. Spectroscopic detection along the length of the tube, or mass spectrometry at the end of the flow tube, using a moveable injector to vary the flow distance, is the most popular detection method.

2.4.4 Mixing Configurations

Different mixing configurations have been studied by Mullin (2001). Figure 7 illustrates two reactant addition methods commonly used applied to reaction systems, namely, 'single jet' and 'double jet'. In single jet mode, reactant B is already in a vessel and reactant A is either fed on the surface or into agitated zone near the impeller. The latter being preferred for formation of larger precipitates as better mixing reduces the level of local supersaturation and minimise nucleation rate. In double jet mode, reactant A and B are simultaneously added on surface, at impeller tip or premixed and fed into reactor as a single stream.

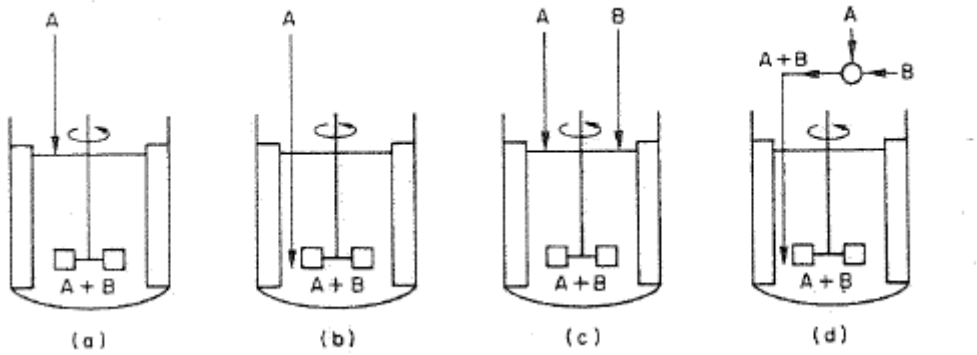

Figure 7: Reactant addition Methods

The choice of the best mixing configuration is based how well the reactants are mixed and the quality of the products to be formed. The method and sequence of mixing reactants into the reactor determines the particle size distribution, crystal habit, polymorphic modification, crystallinity, purity and degree of agglomeration of precipitates during purification processes.

3 LITERATURE REVIEW

Many factors have been proposed to affect the feasibility of selective metal sulphide precipitation from multi-metal ionic systems. Although literature covers a wide variety of these, this review focusses on the importance of controlling pH, concentration and addition of sulphide ions, seeding and influence of different mixing configurations on selectivity, particle size and morphology. Although the literature presents these factors in different contexts, the primary focus is on their applicability to purification of hydrometallurgical streams.

3.1 Metal Sulphide Purification Chemistry

The general reaction for purification of hydrometallurgical streams using metal sulphide precipitation involves the pH dependent sulphide speciation and the reaction of the dominant sulphide species with the metal ions to form a sparingly soluble metal sulphide precipitate. According to Jackson (1986), the aqueous speciation of sulphide is shown by the dissociation reaction Equations 3.2 and 3.3. Equation 3.4 summarizes the interaction of the metal impurity with the sulphide source for the formation of a metal sulphide precipitate.

$$H_2S_{(aq)} \leftrightarrow HS^-_{(aq)} + H^+_{(aq)} \quad 3.2$$

$$HS^-_{(aq)} + H^+_{(aq)} \leftrightarrow S^{2-}_{(aq)} + 2H^+_{(aq)} \quad 3.3$$

$$Me^{2+}_{(aq)} + HS^-_{(aq)} \leftrightarrow MeS_{(s)} + H^+_{(aq)} \quad 3.4$$

This is only achievable when the ionic product of the target metal sulphide exceeds the solubility product constant. Thus, a control of the concentration of sulphide ions to metal ions and the operating pH are of paramount importance during the purification process.

3.1.1 pH control

The pH of the reacting solution is very significant for selective metal sulphide precipitation. As indicated in Equation 3.2 and 3.3, the speciation of the sulphide (HS^- and S^2) is highly dependent on the pH of the solution. According to Jackson (1986), for a gaseous hydrogen sulphide of saturation concentration 0.09 mol L^{-1} in water under a partial pressure of one atmosphere at 25^0C, the pH of the solution is directly related to the sulphide ion concentration by Equation 3.5 below. Increasing pH by one level increases the ion sulphide concentration by two orders of magnitude.

$$\text{Iog } [S^{2-}] = \text{Iog } 8.4 \text{ x } 10^{-26} + 2\text{pH} \qquad 3.5$$

Migdisov (2002) explored pH-dependency of aqueous sulphide speciation and summarized finding as illustrated in Figure 8.

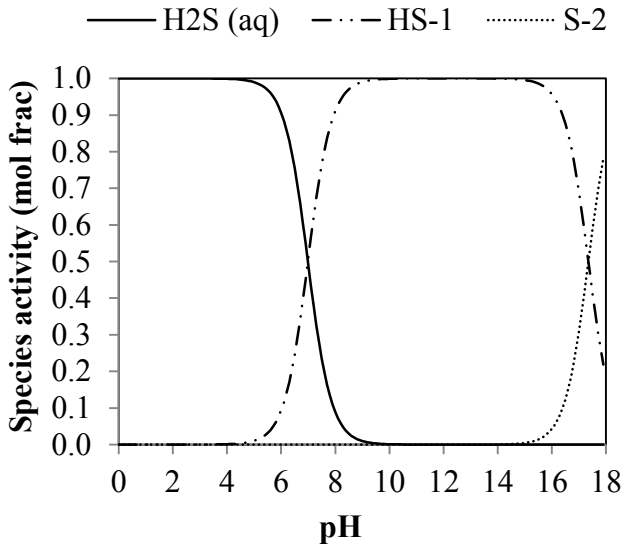

Figure 8: pH dependency of hydrogen sulphide speciation

Accordingly, Hammack et al (1994) observed that at low acidic conditions the rate of dissolution of H_2S was low, limiting the concentration of HS^- ions available for precipitation. At neutral to alkaline conditions, Rickard's (1995) studies on identifying the reaction pathway for iron (II) sulphide reported a bisulphide mechanism where the formation of $Fe(HS)_2$ was dominant. Since hydrogen ions which are continuously formed in this critical region, lower the pH to levels that promote the dominant speciation of H_2S in solution over

that of the HS^- and S^{2-} ions, an alkaline source has to be continually added to raise the pH and maintain optimal HS^- speciation. Also, the sulphide ions rarely exist at significant concentrations in aqueous solutions (Stumm & Morgan, 1996).

Evidence that the pH changes during sulphide precipitation was supported by the dominant reaction pathway. This was first proposed by Kolthoff and Moltzau (1935) who reported a two-step mechanism which involved the reaction of bisulfide ions to initially form the metal hydrosulphide which, by secondary loss of protons, (H^+ ions), resulted in the formation of the metal sulphide itself. According to Joris' (1969) studies on rates of precipitation, after induction time intermediate, compounds of Ni $(HS)_2$ and Co $(HS)_2$ were formed which later transformed to precipitates of NiS and Co_9S_8. This conception was later confirmed by Hammack et al (1994), Lewis and van Hille (2006) and Karbanee et al (2008) and can be summarized by Equation 3.6 and 3.7 below.

$$Me^{2+}{}_{(aq)} + 2HS^-{}_{(aq)} \leftrightarrow Me(HS)_{2\,(aq)} \qquad 3.6$$

$$Me(HS)_{(aq)} \leftrightarrow MeS_{(s)} + H^+{}_{(aq)} \qquad 3.7$$

Early studies on purification of manganese (II) sulphate electrolyte in an ammoniacal solution proposed that an intermediate compound, Mn (HS^-) was initially formed. This subsequently proceeded to either form MnS or further reacted with the metal impurities, Me^{2+} ,to form sulphides of MeS (Harris, Meyer & Auerswald, 1977). The analogous reaction using ammonium sulphide instead of gaseous hydrogen sulphide would then proceed according to Equation 3.8-4.1.

$$(NH_4)_2S_{(aq)} \leftrightarrow 2NH_{3\,(aq)} + H_2S_{(aq)} \qquad 3.8$$

$$2NH_{3\,(aq)} + H_2S_{(aq)} \leftrightarrow 2\,NH_{3(aq)} + HS^-{}_{(aq)} + H^+{}_{(aq)} \qquad 3.9$$

$$2Mn^{2+}{}_{(aq)} + 4HS^-{}_{(aq)} \leftrightarrow 2Mn(HS)_{2\,(aq)} \qquad 4.0$$

$$Mn(HS)_{2\,(aq)} + 2Me^{2+} \leftrightarrow 2MeS_{(s)} + Mn^{2+}{}_{(aq)} + 2H^+{}_{(aq)} \qquad 4.1$$

The aqueous ammonia produced in Equation 3.8-3.9 would possibly act as a buffer against the increase in acidity of the precipitating solution, permitting the formation of metal sulphides to proceed to completion unlike a case where only hydrogen sulphide is used.

The competitive precipitation reactions described in Equation 4.0-4.1 may proceed by heterogeneous cationic substitution where the formed $Mn(HS)_2$ formed may further release the bisulphide ion to promote precipitation of the most soluble metal sulphide at that particular pH level mainly due to difference in sulphide solubilities.

Figure 9 illustrates the relationship between pH and the solubility of metal sulphides (Lewis, 2010).

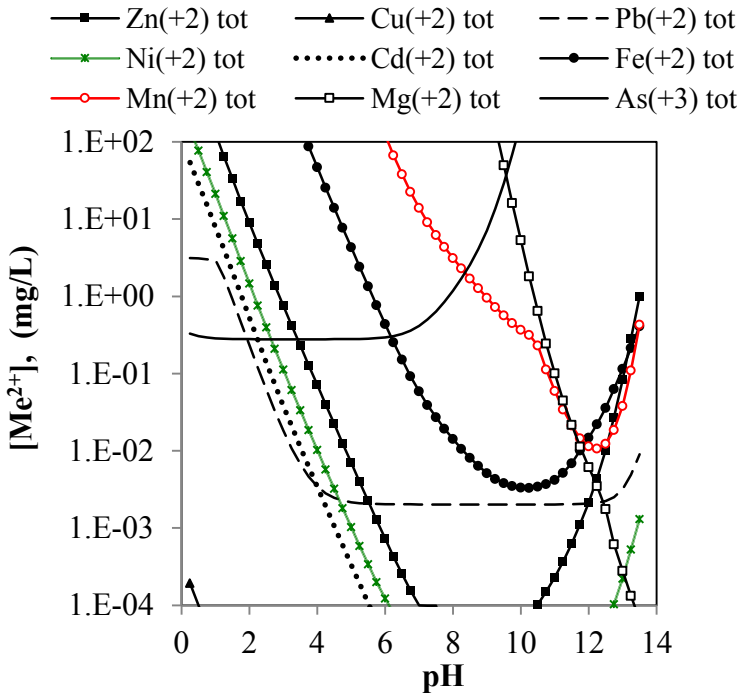

Figure 9: pH dependency of metal sulphide solubility ((Lewis, 2010)

These thermodynamic curves have been exploited to predict the potential for selectivity, predict the operating pH and extent of precipitation of metal ions during purification of simple and complex hydrometallurgical streams. Generally metal ions such as copper, lead and arsenate would readily precipitate to form insoluble metal sulphides at low pH conditions while manganese and magnesium form at higher alkaline pH levels. Selective separation of cadmium, nickel and zinc ions may be difficult as they exhibit similar solubilities throughout the critical pH levels. This data also proves that sulphide precipitation achieves extremely

low residual concentrations which tie with the necessary limits required in hydrometallurgical processes. For instance, Figure 10 illustrates the chemical equilibrium diagram obtained with the OLI Analyser Studio 9.0 Software for a typical manganese (II) sulphate electrolyte.

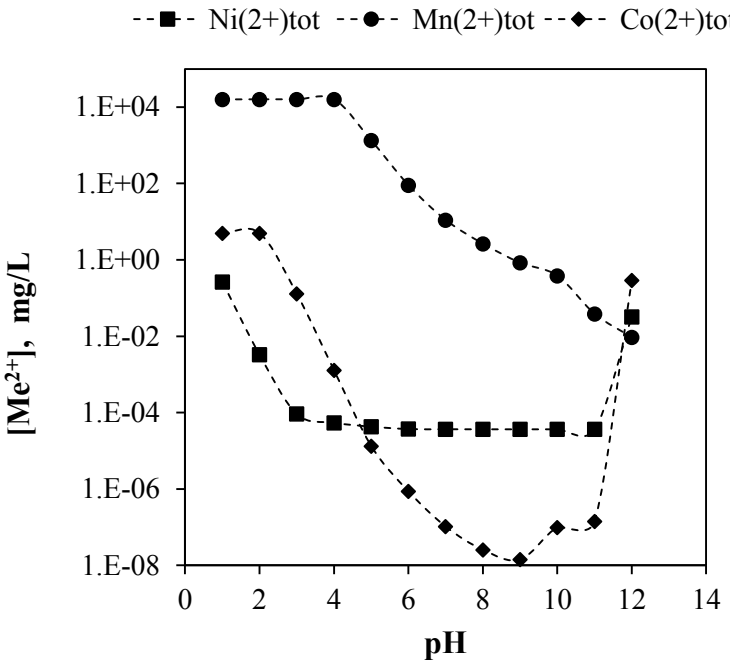

Figure 10: pH dependency of CoS, NiS and MnS (OLI stream analyser)

Briefly, selective removal of each of the impurities of CoS and NiS is nearly impossible as the solubilities are closely similar for each pH level. These can only be successfully removed from this system as mixed sulphide. Although operating at pH levels between 6.8-7.5 is commonly used in industrial practices (Wanamaker & Morgan, 1943; Bryson & Bijsterveld, 1991; Lewis, Nathoo & Gluck, 2006; Karbanee, van Hille & Lewis, 2008), there is a compromise between losing desired manganese ions, through co-precipitation ,and achieving ideal residual concentration of impurities to levels below 1ppm.

Adjusting the initial pH of the solution to between 1.7-3.9 and operating at elevated pressures, selectively removes NiS from such a multi-metal ionic system (Jha, Wicker & Meyer, 1978). This observation was recently supported by Cibati et al (2013) who validated a thermodynamic prediction obtained with Medusa Software 32. The model was developed for a system of Co-Ni-V-Mo in biogenic H_2S and NaOH. They selectively formed mixed Co-Ni sulphides at pH levels as low as 3.5.

Although operating at low pH achieves selectivity, the speciation of gaseous H_2S is limited. Hence, precipitation can only be facilitated by altering its solubility by either increasing temperature, pressure or in some cases including a catalyst. Huggin et al's (1978) investigation into the precipitation of filterable nickel and cobalt sulphides proposed that at low pH levels gaseous H_2S can achieve a maximum efficiency of 77% at a temperature of 75^0C. Although higher temperatures achieved an advantage of producing fine precipitates of satisfactory bulk density and settling rate, the efficiency of H_2S dropped considerably with excessive evaporation of corrosive liquids and limitations of open, temperature sensitive reaction vessels. Crundwell and co-workers (2011) reported that this theory was later adopted by a number of companies such as Murrin Murrin, Coral Bay and Ravens Thorpe BHP Billiton who achieved + 99.99% removal efficiency for CoS and NiS by operating between pH levels of 1.5-3.5. Their purification process was conducted in autoclaves and the toxic gaseous hydrogen sulphide's solubility was altered by operating at elevated temperatures of 80-120 ^{0}C, pressures of 2-10 bars, residence times of 1-2 hours and seeding through a recycle stream. However this renders this process economically unviable due to the associated high capital and operating costs.

Numerous other studies dating back to 1970s have successfully used the pH dependent solubility of different metal sulphides to selectively remove metal ions from multi-metal ionic systems. No literature on these studies was found for the period 1980-1990. Early work by Jha et al (1978) selectively precipitated nickel and cobalt sulphides from solutions of the leached laterite ores. Their observations indicated that the higher the initial pH, the lower the residual metal ion concentration and the lower the reaction time for achieving approximately 99% precipitation efficiency.

In recent years, problems associated with the treatment of acid mine drainage have triggered the interest of most researchers resulting in many publications on the subject topic. Tabak et al (2003) successfully precipitated CoS, ZnS, FeS and MnS selectively and sequentially from an AMD stream using biologically produced H_2S. Although this process was able to demonstrate very high precipitation efficiency of CoS (99.1%), ZnS (100%), FeS (97.1%) and MnS (87.4%) and precipitate purities above 70%, this was achievable through six staged units. Similarly, conclusions by Cibati et al (2013) promoted the use of biogenic H_2S for selective precipitation from a Mo-Ni-Co-V system. However, at pH 3.5, the average recovery for a mixed nickel and cobalt sulphide was only 18.5% with an equally poor purity index.

Likewise, despite the use of the generic sodium sulphide reactant, Fukuta et al (2004) asserts that selectivity is feasible for a Cu-Ni-Zn system. Selectivity was achieved at 94% for CuS at a pH range of 1.4-1.5, 75 % for ZnS at pH range of 2.4- 2.5 and 65% for NiS at pH range 5.5-6.0. These relatively compare to findings by Kondo et al (2006) and Tokuda et al (2008), who additionally reported an increase in selectivity, owing to more a precise control of pH for precipitation of each metal sulphide.

However, a pH cascade suggests that the separation for each metal ion can only be achievable in separate units. This may be difficult in practice due to the cost associated with setting up a number of process units and the associated control of different fluctuations on the initial operating conditions.

3.1.2 Sulphide Concentration

Sulphide precipitation is commonly effected using either aqueous, (Na_2S, NH_4S and NaS) or solid (FeS and CaS) or gaseous H_2S or through degeneration of sodium thiosulphate. Although early studies showed that the application of Na_2S for sulphide precipitation was highly effective for lowering concentrations of Cd^{2+},Cu^{2+} and Zn^{2+} to less than $0.1 mgL^{-1}$ (Bhattacharyya et al., 1981), ammonium sulphide is widely used in hydrometallurgical process for its additional buffering properties. Recent studies prefer the use of gaseous hydrogen sulphide in an attempt to reduces the rate of generation of supersaturation by exploiting the mass transfer limitation of its dissolution (Lewis & van Hille, 2006).

Chemical equilibrium diagrams are usually used to determine the precipitating order of metal ions according to the suphide ion concentration and the pH. Figure 11 illustrates a typical sulphide solubility diagram. It can be noted that the solubility line for Mn^{2+} is extremely far to the right side of the diagram ,indicating that MnS is more soluble than CoS and NiS. This offers a theoretical basis for separation of Co^{2+} and Ni^{2+} from a system of Co-Ni-Mn. Furthermore, it was observed that the exchange rates correspond to the value of the solubility products of fresh, amorphous metal sulphides(Wu & Yang, 1976). Accordingly an increase in concentration of sulphide ions results in rapid increase of metal removal rate in the precipitation order of Cu > Pb > Cd > Zn, thus the order of solubility of metal sulphides. This

selectivity is attributed to differences in metal sulphide solubilities (Villa-Gomez et al., 2012).

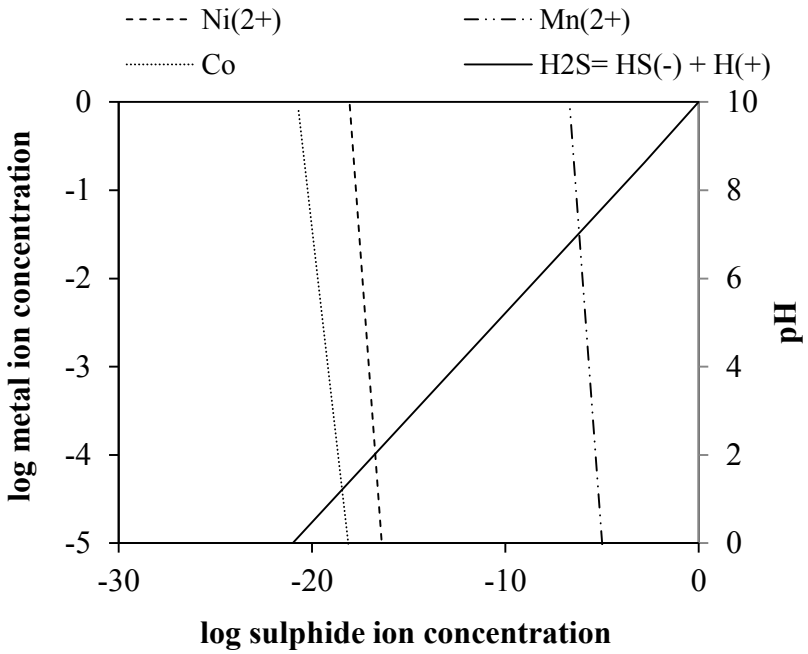

Figure 11: Sulphide solubility diagram at 25 ^{o}C

Studies on effect of sulphide concentration on multi-metal ionic systems have proven that an amount of H_2S equi-molar to that of the metal ion is sufficient to achieve complete precipitation. Lewis and van Hille (2006) studied the effect of a reagent ratio on precipitation efficiency and conversion for a Co-Ni system, the result indicated that a stoichiometric ratio of 1:1 for metal ion to sulphide concentration, immediately precipitated NiS and CoS and achieved metal removal efficiency of 99.8% for Co^{2+} and 99.9% for Ni^{2+}. However, these sulphides re-dissolved into solution as polysulphide complexes, despite the continued decrease of free sulphide in solution.

Figure 12 shows the changes in concentration of Co^{2+} and Ni^{2+} ions with time. This graph indicated that decreasing the reagent ratio compromised the metal removal efficiency. Excess sulphide ions concentrations, promoted the formation of soluble polysulphide complexes (Karbanee, van Hille & Lewis, 2008; Mokone, van Hille & Lewis, 2009) and inhibited precipitation to very low levels by purely solubility considerations. This was also consistent with the observation that no significant quantities of aqueous sulphide species were recorded

after precipitation, despite the initial stoichiometric excess. These complexes were also found to be stable at low HS^- ion concentrations less than 10^{-6} M (Shea & Helz, 1988).

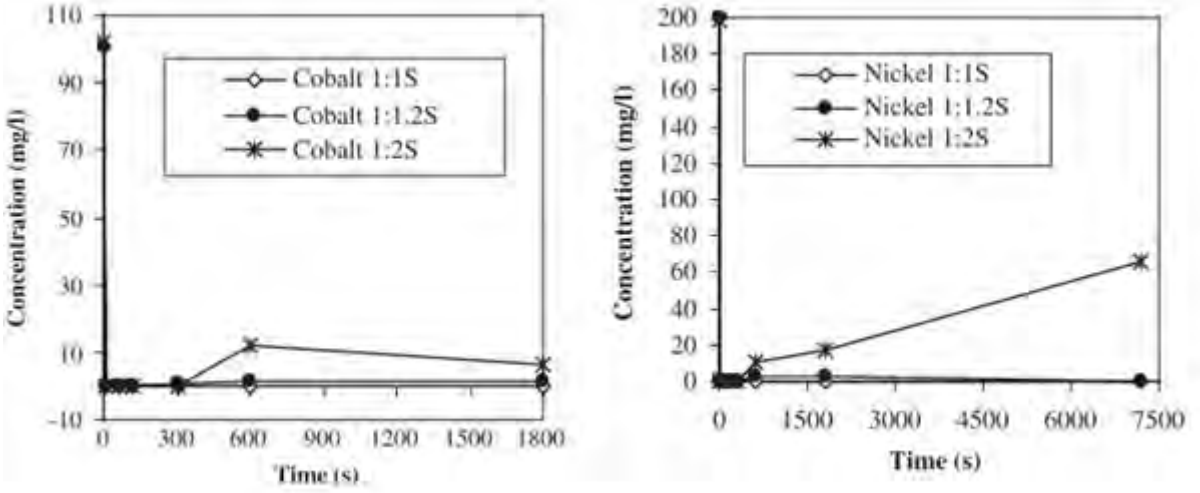

Figure 12: Nickel and cobalt concentrations in the batch experiments using aqueous sulphide source

Furthermore, the reagent ratio strongly influences the characteristics of precipitates formed in terms of particle size and morphology. At high sulphide concentration, a significant amount of fine amorphous metal sulphide particles are formed.

3.2 Mechanisms of Co-precipitation Purification

Literature on mechanisms of purification of hydrometallurgical systems is very limited to before 1970s, particularly that specific to the Co-Ni-Mn sulphide co-precipitation system. Although many kinetic studies have been performed on similar systems, information on the mechanisms is yet to be confirmed.

The main mechanisms of purification from multi-metal ionic systems include the classic, ionic precipitation, adsorption precipitation and heterogenous cationic substitution.

3.2.1 Adsorption Precipitation

Kolthoff (1931) proposed a theory of co-precipitation and argued that metal sulphide precipitates are always contaminated by adsorbed ions. He later confirmed that this ‘induced

co-precipitation' was because of the strong adsorbent properties of colloidal metal sulphides towards H_2S, HS^- and S^{2-} (Kolthoff & Moltzau, 1935).

This mechanism promotes the simultaneous removal of both the least and most soluble metal ion from solution under conditions where the most soluble would not precipitate or where the concentration of metal ions is insufficient to exceed the solubility product of the other. This is supported by the Paneth Fajans Hahns' adsorption rule which on application suggests that if copper sulphide is in contact with a solution in excess of sulphide ions it would adsorb ions in the order of Zn > Co > Ni > Fe > Mn. This reflects the order of solubility of respective metal sulphides ZnS < CoS < NiS < FeS < MnS.

The induced precipitation processes is achieved when the cations replace the hydrogen ions in the H_2S that is adsorbed on the metal sulphide, releasing a corresponding amount of acid. Thus, the precipitation rate on the surface would increase due to domination of crystal growth over primary nucleation. In support of this, an observation by Salutsky et al (1959) suggested that if cobalt sulphide is precipitated from a solution containing excess sulphide ions and metal ions, sulphide ions will be adsorbed during growth of the precipitate and drag cations to the surface. On the other, hand if excess cobalt ions are in excess during growth, anions will be adsorbed and co-precipitate with cobalt sulphide, unless mixed precipitates are formed.

Since, surfaces of metal sulphides are active; ions are incompletely coordinated and are free to attract other ions of opposite charge from the solution. The ionic charge and ion size determines the effectiveness of electrostatic attractions on the surface of a precipitate. For example, for an ionic charge of (+2), at a low spin, the ionic radii is 74 pm, 79 pm and 81 pm for cobalt, nickel and manganese ions respectively. Hence, these can easily co-precipitate by adsorption.

A number of factors affect co-precipitation by surface adsorption. A high concentration of impurity increases probability of solute interaction at the precipitate surface and promote adsorption. Adsorption is also controlled by altering the concentrations during precipitation or aging the precipitates to promote particle growth and reduce surface area. Furthermore, altering the pH level of the solution reduces the effects of this mechanism.

Although studies in the 1970s and before, acknowledge that while adsorption is necessary for the precipitation processes of multi-metal ionic systems, it is not the only process responsible for the removal of cations during precipitation. This was confirmed by Lewis et al (2006) who concluded that the removal mechanism of cobalt and nickel from an electrolyte occurs by a combination of precipitation reaction and adsorption. In their study, adsorption accounts for approximately 30% of the nickel ions and 58% of cobalt ions that are removed from solution.

Other possible mechanisms include occlusion and inclusion. Occlusion is when the impurity within a precipitate is mechanically entrapped by subsequent crystalline layers. This is more prevalent in freshly prepared colloidal metal sulphides and hydroxides precipitates due to their large surface areas. Mechanical entrapment is promoted at high localized supersaturation and spontaneous nucleation processes. However, some of the metal ions are involved in the interior of the crystal and form part of the crystalline structure or form between layers. These are difficult to remove by most of the mentioned methods above due to passivation of metal sulphides.

3.2.2 Cationic substitution

McGeorge et al. (2009) identified heterogenous cationic substitution as an alternative co-precipitation. The basis of this investigation was that both thermodynamic and kinetic effects dominate selective purification when the difference in the metal ion concentrations is very high.

In an attempt to selectively precipitate Rh^{3+}, of a concentration two orders of magnitude lower than that of the least soluble Cu^{2+} ions in the system, the metal ions initially competed for the sulphide ions through ionic precipitation. The formation of CuS is favoured due to the faster reaction rate compared to that of the Rh_2S_3. The large difference in the solubility products later provides a chemical driving force that promotes the removal of Rh^{3+} ions via cationic substitutions. Again, the extent of precipitation of Rh^{3+} may be due to passivation of CuS (McGeorge, Gaylard & Lewis, 2009). Recent studies have taken advantage of this mechanism and have successfully used amorphous MnS to selectively remove copper ions from a nickel electrolysis anolyte at an industrial scale (Li et al., 2014). Similarly, if

manganese (II) sulphate electrolyte was purified to remove cobalt and nickel ions through cationic substitution mechanism, the MnS would initially be precipitated out then exchange cations with Co^{2+} and Ni^{2+}, in the order of their differences in solubility product

3.3 Reaction Kinetics for the Purification Process

Numerous studies have been performed on reaction kinetics for multi-metal ionic systems. The difference in reaction rates for precipitation of each metal sulphide usually forms a basis for selective separation through ionic precipitation.

Bryson and Bijsterveld (1991) investigated the reaction kinetics during purification of manganese (II) sulphate electrolyte containing cobalt ions as the main impurity. The concentration of the manganese ions in the stream was three orders of magnitude lower than that of the cobalt ions. Findings showed that the precipitation of CoS exhibited three kinetic regions, an induction period that was followed by rapid reaction rates then a slow approach towards equilibrium. The induction period was eliminated completely by catalysis using combined manganese and cobalt sulphides; this is illustrated in Figure 13.

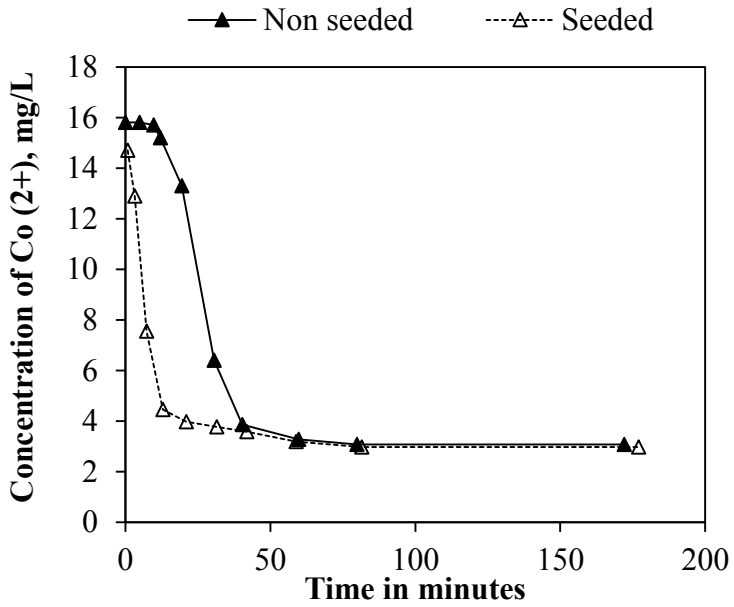

Figure 13: Concentration changes of Co^{2+} ions during purification of a Co-Mn system

However, the rate of reaction for MnS co-precipitation was first order, of which, the corresponding change in concentration with time is given in Figure 14. This was in

accordance with the findings of Mishra and Das (1992) during the purification of zinc electrolyte.

On the contrary, Lewis and Swartbooi (2006) found that, using a batch reactor, the kinetics of nickel and cobalt sulphides ,from a Co-Ni system were first order with respect to both metal and sulphide concentrations. The nickel sulphide precipitation reaction was reported to be twice as fast as that of the cobalt sulphide reaction, (k_{ni}= 5.8 $M^{-1}s^{-1}$ and k_{co}=2.2 $M^{-1}s^{-1}$). No induction period for cobalt sulphide kinetics was noted. The lack of an induction time for the cobalt was attributed to the presence of the nickel sulphide precipitates, which acted as heterogeneous nuclei. However, the concentrations levels investigated were not for a typical industrial electrolyte, relatively similar concentrations of metal ions were used to make the Co-Ni system.

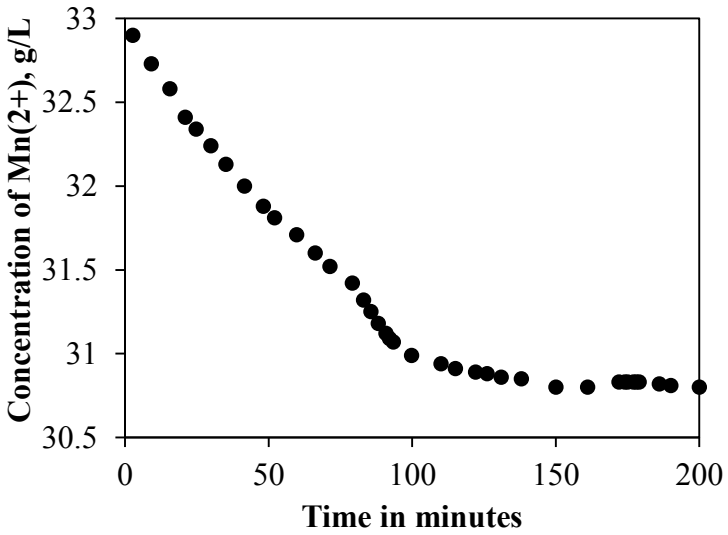

Figure 14: Concentration changes of Mn^{2+} ions during purification of a Co-Mn system

Tokuda et al (2008) also studied the reaction kinetics for a single metal system and a multi-metal ionic system of Cu-Zn-Ni system using gaseous hydrogen sulphide. They additionally reported that the reaction rate constants obtained from precipitating a single metal stream with sulphide ions were similar to those from a multi-metal ionic of Cu-Zn-Ni stream. For instance, direct precipitation of NiS from a single metal ion stream had a reaction rate constant of 6.23 $x10^{-4}$ s^{-1} compared to 5.63 x 10^{-4} s^{-1} attained from the precipitation of the same metal sulphide from a Cu-Zn-Ni system. Therefore, this suggested that the influence of metal ion interaction does not have a significant effect on the precipitation kinetics of nickel

sulphides. These reaction rates constant suggest that these precipitation reactions are very fast.

3.4 Hydrodynamics

The rate of precipitation of cluster complexes of metal sulphides of Cu, Zn, Ag and Pb ions was calculated and it was concluded that their reaction rate constants were greater than 10^8 $M^{-1}s^{-1}$ (Luther & Rickard, 2005). This suggests that, to obtain an accurate measurement of the reaction kinetics for such a sparingly soluble sulphide, there is need to use a highly sensitive detection method and the precipitating apparatus should achieve a mixing time that is less than the reaction time for any of the metal ions to be precipitated. A case study is illustrated in Figure 15.

It shows that the nucleation time is faster than any of the mixing times, thus reaction kinetics measured for such a precipitation process is mixing limited (Baldyga & Pohorecki, 1995). Complete mixing for fast kinetics is ideally achieved within milliseconds, shorter than the reaction time or appearance of first nuclei.

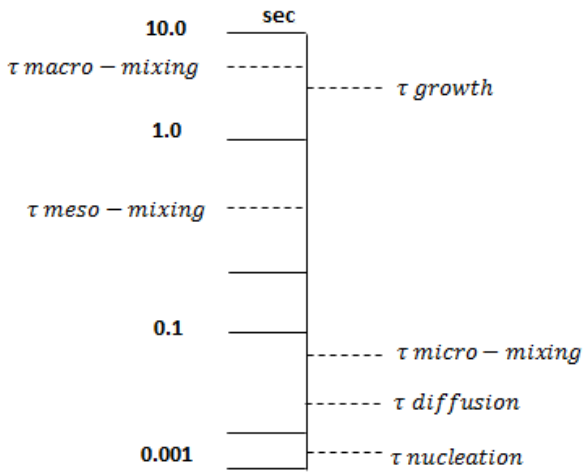

Figure 15: Reaction time and mixing times scales

3.4.1 Mixing

Metal sulphide precipitation reactions are commonly conducted in classic stirred reactors or Mixed Suspension, Mixed Product Removal reactors (MSMPR). The level of supersaturation produced at different locations within such reactors varies due to the non-symmetry of the turbulent velocity field necessary for bulk convective mixing for solid-liquid phase systems, (Vicum et al., 2004). This affects the characteristics of the precipitates and their product quality. Over the years, a number of alternative reactor technologies have been proposed for precipitation of sparingly solid precipitates. These include fluidised bed reactors and bubble column reactors (Lewis & Swartbooi, 2006). However, the hydrodynamics of these systems are very complex.

Lewis and Swartbooi (2006) compared properties of metal sulphide precipitates at various supersaturations using different batch stirred reactor, seeded fluidized bed and semi batch bubble column reactors. They reported significant quantities of fines of sulphide precipitates from all the three reactors at both low and high supersaturations (Bryson & Bijsterveld, 1991). This is proposed to be due to homogenous nucleation and attrition.

Developing work (Rickard, 1989; Roelands et al., 2003; Chiang, Nathoo & Lewis, 2007; Kugler, Doyle & Kind, 2014) has confirmed that the Y and T-mixers are preferred choices for better mixing and good product quality. The use of micro-mixers has been largely adopted for investigating precipitation kinetics, (Rickard, 1989; Roelands et al., 2003), nanoparticle precipitation, (Gradl & Peukert, 2010), and reactive polymerization precipitation. Furthermore ,these technologies ensure reproducibility and stability in continuous mode compared to stirred tank reactors which are difficult to scale up as small changes in internal geometry may lead to large variations in mean crystal sizes. There is also control over initial supersaturation and complete mixing is achieved within milliseconds (Benet et al., 2002). However, one main disadvantage is that it usually requires use of lots of reactants.

Chiang et al (2007) studied the effect of using various mixing configurations on control of particle size distribution during manganese sulphide precipitation. They reported that at low supersaturation levels, the T-mixers are more effective in forming small particles of manganese sulphide precipitates of a narrower size distribution compared to the different angled Y-mixers and stirred tank reactors. It was also noted that aggregation mechanism

dominates these kinds of micro-mixing processes. The geometry of these systems also resulted in a steady state being established in the apparatus making it more suitable for monitoring a detailed progress of a reaction and at high measurement precision and accuracy (Rickard, 1989).

Micro-mixing affects the course of rapid and instantaneous chemical reaction, changing their conversion and selectivity (Baldyga & Pohorecki, 1995). Performing precipitation at low supersaturation and feeding reactants at a point of intense mixing, near the impeller as far apart as possible promotes good dispersion of reactants in the reactor vessel. This also obtains large particle sizes of narrow distribution and high crystallinity (Grulietti et al., 2001). Additionally, Nienow and Inove (1993) studied the selectivity for a by-product at different feed points in the reactor using different types of impellers. Findings indicated that for all cases, high selectivity was achieved when reactants were fed parallel to each other, at the tip of the impeller. Poor selectivity was reported when feeding was done at the top or bottom of the reactor away from this impeller.

3.5 Industrial Applications of Metal Sulphide Precipitation

Commercially, metal sulphide precipitation is employed for selective removal of metal ions from multi-metal ionic streams during purification of hydrometallurgical streams. Amongst many, these include purification of manganese (II) sulphate electrolyte from impurities of cobalt, nickel and iron ions (Wanamaker & Morgan, 1943; Jacobs, 1946; Bryson & Bijsterveld, 1991) ,separation of cobalt ions from an ammoniacal stream of zinc (II) sulphate (Mishra & Das, 1992), competitive removal of rhodium (III) ions (McGeorge, Gaylard & Lewis, 2009) and recently, that of selenium ions (Mokmeli, Wassink & Dreisinger, 2013) from acidic copper sulphate electrolyte. Most commonly, selective sulphide precipitation is applied for separation of platinum group metals (Siame & Kasaini, 2013) and for economic recovery, reuse of valuable metals and for minimization of toxicity in waste streams prior to disposal into the environment (Sahinkaya E. et al., 2009; Kamal et al., 2011; Gharabaghi, Irannajad & Azadmehr, 2012; Cibati et al., 2013; Reis et al., 2013).

3.6 Research Motivation

Previous research work acknowledges the effect of supersaturation, sulphide dosing and pH on selective removal of metal ions from multi-metal ion systems. However, these were largely studied for systems with relatively equal and small concentrations of metal ions in the multi-metal ionic stream. The focus was also on removal of only one metal impurity at one given stage, each operated at different conditions. Hence, the conclusions of these findings may not directly relate to a typical hydrometallurgical system where the concentrations of impurities are not only several orders of magnitudes lower than that of the target metal but the solubility products of the metal impurities are also closely related challenging the sequential separation. This would be due to competitive interaction of metal ions during the purification process. Although purification of systems of Co-Mn, Co-Ni and Ni-Mn have been reported, these also do not further acknowledge the possible influence of operating factors on removal of two or more impurities from a multi-metal ion stream. The separation through a number of stages in economical unviable and is not an option for industrial processes.

This research seeks to contribute towards bridging the gap between fundamentals and practical aspects in metal sulphide based purification of hydrometallurgical systems. This is important in developing an understanding into the relationship between mixing configurations, operating conditions and selective removal of impurities. The main objective was to understand the influence of local supersaturation on simultaneous selective removal of two impurities, extending the approach of using a T-premixed reactor to achieve perfect mixing, control levels of supersaturation and produce particles of a narrower PSD.

The outcome of this research would go a long way towards modelling, designing and developing efficient processes of minimal operating costs. Existing operations can also use this knowledge to optimize their processes and improve productivity. Moreover, this can also be adopted for selective recovery of metals in extremely low concentrations.

3.7 Research Hypothesis

The following hypotheses were tested in this study:

1. A decrease in the micro-mixing time for sulphide precipitation results in an increase in selective removal of Co^{2+} and Ni^{2+} ions from a Co-Ni-Mn system. This is due to increased precipitation rate of these metal impurities as mixing time approaches their reaction time.
2. Increasing the pH of the reacting solution improves selective removal of Co^{2+} and Ni^{2+} ions from a Co-Ni-Mn system by altering the reactivities of metal ions. However, this increase is limited to pH levels of up to 7.1, beyond which, sulphide precipitation of these metal ions co-precipitates with Mn^{2+} ions.

3.8 Research Objectives

This research project seeks to understand the influence of local supersaturation on selective removal of NiS and CoS during purification of manganese sulphate electrolyte, using an ideally mixed system.

Therefore, the research objectives of this study are as follows:

1. To investigate the effect of mixing configuration on PSD, morphology and on selective removal of CoS and NiS from Co-Ni-Mn system.
2. To investigate the effect of pH on selectivity for CoS and NiS from a Co-Ni-Mn system, using a suitable mixing configuration identified in (1) above.
3. Investigate the possible mechanism for selective removal of CoS and NiS from a Co-Ni-Mn system.

3.9 Key Research Questions

The following key questions have been formulated:

a) Does mixing in a semi-batch stirred tank reactor and T- premixed affect selectivity for CoS and NiS in any way?

b) How does the control of supersaturation in relation to mixing configuration affect the size and morphology of precipitated particles?

c) At what operating pH levels can you achieve residual impurity levels below 1 ppm?

d) What is the batch time necessary for achieving high selectivity for impurities with minimum co-precipitation of manganese ions?

4 MATERIAL AND METHODS

This chapter gives a detailed description on thermodynamic models, reagents and equipment, experimental procedures and analysis techniques used in this study.

4.1 Experimental Design

The investigation was divided into three main sections. Firstly, a thermodynamic model was done to confirm the feasibility to selectively remove metal impurities of CoS and NiS from a system of Co-Ni-Mn and thus, identify the operating pH boundaries for this study. Secondly, preliminary work was conducted to identify a suitable mixing configuration, offering better selectivity for removal of impurities, to be adopted for the investigation into the effect of varying pH and batch time, on removal of NiS and CoS.

4.2 Thermodynamic Modelling

Thermodynamic modelling in the chemical equilibrium programme, OLI Stream Analyser Studio 9.0.9 was preliminarily done to investigate the feasibility for sequential and selective removal of metal ions, Co^{2+} and Ni^{2+} from a manganese (II) sulphate electrolyte with a typical industrial composition, at varying pH levels. This was important to define the operating conditions for the semi batch experimental work on a stream comprised of all major ions, 5 mg/L Co^{2+}, 50 mg/L Ni^{2+}, 16000 mg/L Mn^{2+}, 16 mg/L NH_4^+, 9.4 x10^{-4} mg/L S^{2-} and 2.8 x10^4 mg/L SO_4^{2-}. The model was allowed to equilibrate at each fixed pH and at a temperature of 35 ^{0}C. The sensitivity of the system for precipitation of CoS, NiS and MnS was tested for pH variations between 1 and 10. Thus, the model assumed that the only metal sulphides with ionic products exceeding solubility products precipitate out of the mixed solution at each pH level.

This modelling was carried out to later compare the predicted thermodynamic result with those obtained experimentally.

4.3 Solution Preparations

Synthetic solutions were prepared for Co^{2+}, Ni^{2+} and Mn^{2+} using Merck chemicals, $CoSO_4.7H_2O$, $NiSO_4.6H_2O$ and $MnSO_4.H_2O$ respectively. A 20% ammonium sulphide solution was diluted and adjusted to equivalent molar concentrations to that of metal ions impurities. De-ionized water was used for all solutions. The actual solution compositions used in the different experimental design phases is summarized in Table 2 below. The concentration of the system was expected to halve when they mix due to the configurations used in this study.

All reagents were bubbled with nitrogen gas of high purity above 99.9% and 0.35 ppm oxygen content, to eliminated possible oxidation of metal sulphides after precipitation by air or oxygen. The temperature of the reactants and that of the reactor contents was maintained at 35^0C for all investigations. The pH of the reacting contents was maintained by dosing 0.1M ammonia/0.1M sulphuric acid solution. A 5% solution of sodium hexa-meta-phosphate was added to samples to disperse agglomerates for efficient PSD characterization.

Table 2: Experimental Solution Composition

Experimental Design	**Solution Compositions, mg/L**			
	Mn^{2+}	**Ni^{2+}**	**Co^{2+}**	**S^{2-}**
Phase One	1000	1000	1000	1159/2317
Phase Two	32000	100	10	128
Phase Three	32000	100	10	128

4.4 Investigation into the Application of Different Mixing Configurations

4.4.1 Experimental Set up

The aim of this preliminary work was to compare the influence of different mixing configurations on selectivity for NiS and CoS from a system of Ni-Co-Mn. The experiments were carried out in two different semi batch mixing configurations, the double jet stirred tank

reactor (STR) and the T-premixed reactor (TPR), which are schematically illustrated in Figure 16 and Figure 17 respectively. The STR configuration consists of a 1 L jacketed glass STR with a working volume of 0.9 L (0.11 m in diameter), equipped with four baffles. Mixing was achieved by a standard 45° pitched four blade impeller, connected to an overhead variable speed motor which was operated at over 900 rpm.

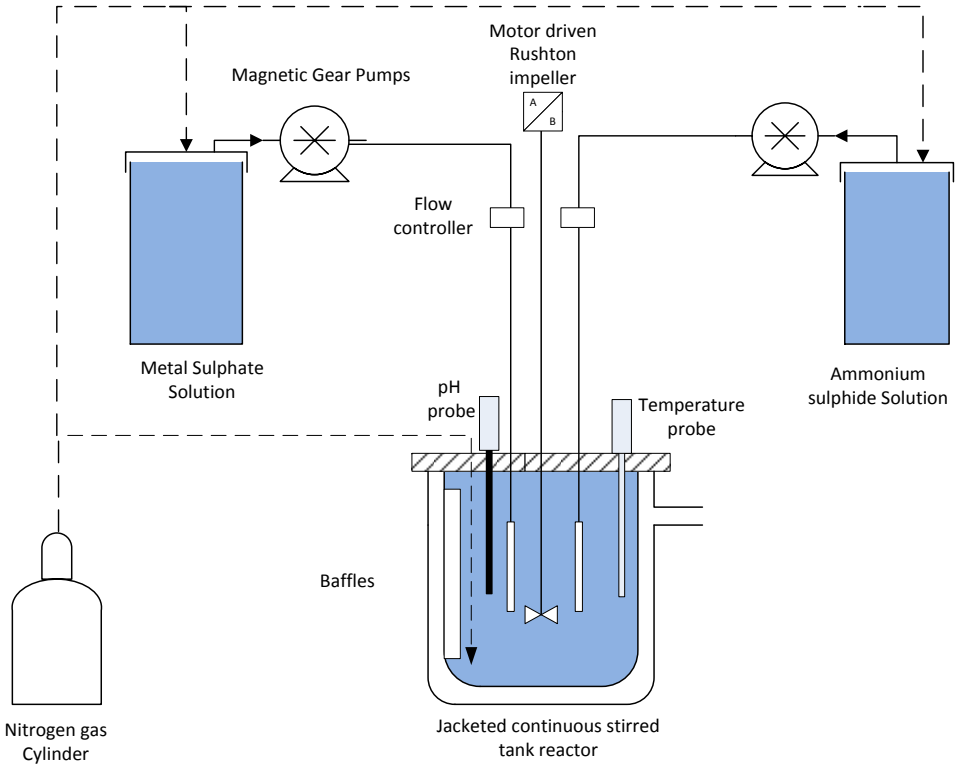

Figure 16: Stirred tank reactor set up

The semi batch STR was fitted with a lid that was used to seal the vessel and hold the sulphide resistant pH probe, temperature probe, overhead stirrer, and two reagents feed tubes parallel to each other, a stainless steel nitrogen injectors and an acid/base dosing port.

The second configuration consisted of a T-premixer, a precipitation tube and a baffled glass jacketed vessel with a working volume of 0.9 L. Mixing was achieved by a standard 45° pitched four blade impeller, connected to an overhead variable speed motor which was operated at over 900 rpm. Design specifications are given in Appendix A.

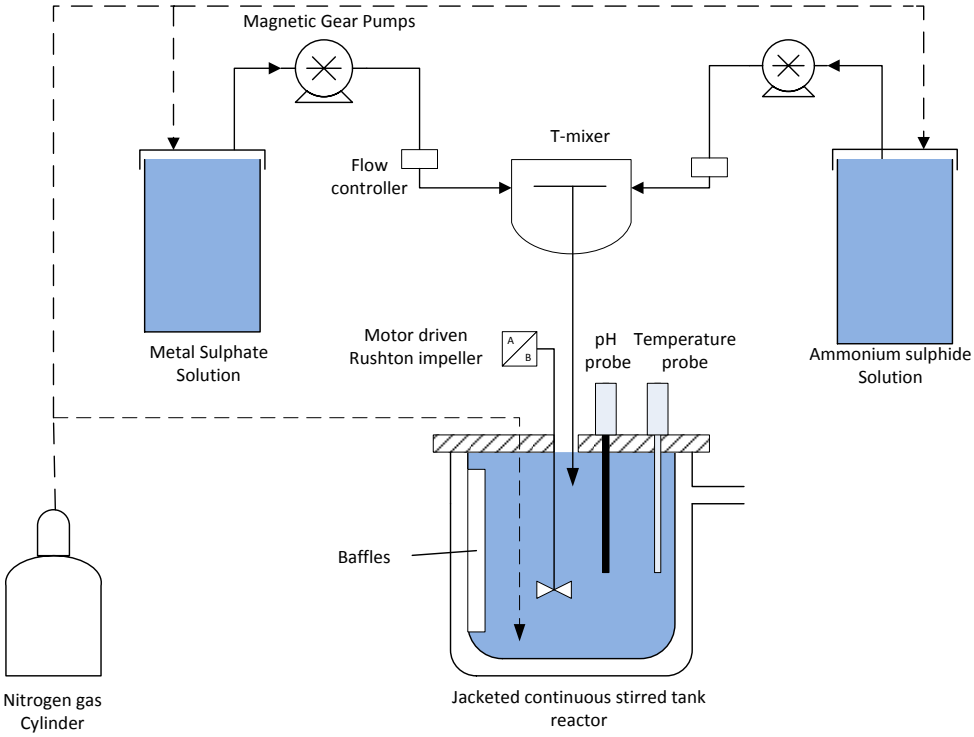

Figure 17: T-premixed reactor set up

The inner diameter of the tubing (D), was 0.004m and the length of the precipitation tube was adjustable to 0.30m. The design specifications of this system were to achieve a fully turbulent flow with a Reynolds number of 6369, mean dissipated rate of 71.4m^2s^{-3} and micro-mixing time of 0.002s. At the end of the precipitating tube, the precipitate was collected in a jacketed stirred vessel which was also fitted with a lid to seal the vessel and hold the sulphide resistant pH probe, temperature probe, overhead stirrer, and two reagents feed tubes parallel to each other, a stainless steel nitrogen injectors and an acid/base dosing port.

In both cases, the feed flows were generated using the calibrated pulseless magnetic gear pumps (Micro pumps). The calibrated sulphide resistant pH probe used was from Metrohm AG (Switzerland). This was also calibrated using Merck Chemicals' standard buffer solutions at pH 4 and 7 before the start of each experiment. The pH was measured every two minutes using a Microprocessor pH meter. The 1 L glass jacketed containers were used to store reactants achieving and maintaining the temperature throughout the experiments.

4.4.2 Experimental Procedure

Both experiments were conducted in a semi-batch system and at a pH level of 7.8. Nitrogen gas was sparged through the reactants for 30 minutes before being pumped into the reactor via the magnetic gear pumps. The flow rate for each reactant was kept constant at 10mL/s for the parallel double jet feed into the STR. Feeding was at a point of intense mixing, near the tip of the impeller as far apart as possible to promote turbulence and good dispersion of reactants in the reactor vessel. On attaining a total volume of 0.9 L, feeding was stopped.

In the same way, one gear pump was used to simultaneously draw the reactants at the same rate, through a T-premixer at 20 mL/s. The reacted metal sulphides were discharged through a tube into the receiving vessel of working volume of 0.9 L.
In both mixing configurations, the time it took to fill 0.9 L batch volume was approximately 45secs. The systems were allowed to equilibrate for one minute after which samples of 25mL were collected after 1,5 and 10 minutes and filtered through a 0.2 μm filter. The filtrate was analysed for free metal ion concentration of Co^{2+}, Ni^{2+}, and Mn^{2+} using the ICP-OES. Part of the sample was analysed for particle size distribution through the Malvern Mastersizer 2000. The filtered solids were washed with a saturated solution of manganese (II) sulphate, dried at 75°C. The dry solid was analysed for morphology through the Scanning Electron Microscopy, and the mineral phase using the XRD analysis. Oxygen contamination of the collected metal sulphide suspension was avoided by sparging nitrogen in the collection vessel.

4.5 Investigation into the Influence of pH on the Purification Process

4.5.1 Experimental Procedure

The pH was measured every two minutes and maintained by addition of 0.1 M ammonia/ 0.1 M sulphuric acid. Table 1 below shows conditions for this investigation, experimental runs were conducted in random, in the order of pH level of 7.8, 4.8, 7.0 and 6.5, to eliminate errors due to uncontrollable deviations. 20mL samples were then collected from the region close to the impeller, at batch residence times of 45minutes. The samples were filtered through a

0.22 μm syringe filter. The filtrate was analysed for free metal ion concentrations of Ni^{2+}, Co^{2+} and Mn^{2+} using the ICP-OES analysis.

Table 1.0: Experimental run conditions

Parameters	**Flow rate (mL/s)**	**pH**	**Temp ^{0}C**	**[Ni^{2+}] (mg/L)**	**[Mn^{2+}] (mg/L)**	**[Co^{2+}] (mg/L)**
	20.0		35.0	100.0	32000.0	10.0
Run 1	✓	7.8	✓	✓	✓	✓
Run 2	✓	4.8	✓	✓	✓	✓
Run 3	✓	7.0	✓	✓	✓	✓
Run 4	✓	6.5	✓	✓	✓	✓

4.6 Determination of the Mechanism of Purification

4.6.1 Experimental Procedure

Using the best mixing configuration identified in Section 4.4 above, this investigation was performed at pH level that were predicted to have minimal co-precipitation with Mn^{2+} ions. The other operating conditions are as described above. Both reactants were heated to achieve a temperature of 35^{0}C before being simultaneously pumped by the magnetic gear pumps through a T-premixer at 20 mL/s and discharged into a batch receiving vessel of 0.9 L.

The reacted metal sulphides were then discharged through a precipitating tube into the continuously stirred receiving vessel. On attaining a total volume of 0.9 L, feeding was stopped. 20 mL samples were then collected from the region close to the impeller, at batch residence times of 45 mins. The samples were filtered through a 0.22 μm syringe filter. The filtrate was analysed for free metal ion concentrations of Ni^{2+}, Co^{2+} and Mn^{2+} using the ICP-OES analysis.

4.7 Measurements and Analysis Methods

4.7.1 Dissolved Metal Ion Concentration

The inductively coupled plasma optical emission spectrometry analysis (ICP-OES) was used to determine the dissolved metal ion concentration. The difference between the initial molar concentrations of metal ions available for reaction, subtract that of the residual metal ions gives a direct indication of the amount of metal sulphide precipitate formed.

4.7.2 pH Measurement

The pH was measured every two minutes using a Microprocessor pH meter. The pH electrodes were calibrated using Merck Chemicals' standard buffer solutions of pH 4 and 7.

4.7.3 Particle Size and Morphology Analysis

4.7.3.1 Scanning Electron Microscopy

Images of mixed metal sulphide were taken using a Scanning Electron Microscopy (Nova NanoSEM 230, FEI). These were obtained using a voltage of 5.0keV, ETD detector (SE mode) with a magnification of between 1000 and 10 000x. These images were used to identify the crystallinity, morphology and particle size distribution of each of the metal sulphides of NiS, CoS and MnS from the mixed precipitate. The images would also help to confirm any possible aggregation associated with the interaction of formed sulphides.

4.7.3.2 Malvern Mastersizer

The precipitates and suspended fine particles were characterised for particle size distribution using laser diffraction Malvern Mastersizer 2000. A few drops of surfactant were added to each sample to avoid possible agglomeration of individual particles and all measurements were conducted within 5 minutes of sampling. The resulting particle size distribution was given as a percentage volume distribution.

4.7.3.3 X-Ray Diffraction (XRD)

Part of the formed precipitate was analysed using XRD. The XRD patterns would then be used to confirm the mineral phase of the precipitated metal sulphides.

4.7.4 Calculation of Precipitated Metal Sulphides

A computation of the concentration of metal sulphides of CoS, NiS and MnS formed at each pH level investigated was performed using Equation 3.7. The initial concentration of each metal ion, $Me^{2+}{}_{(initial)}$, was the composition of these in the Co-Ni-Mn system before reacting with sulphide ions. The residual metal ion concentration, $Me^{2+}{}_{(residual)}$, was tabulated from the ICP-OES analysis of the free metal ion remaining in solution after the precipitation process.

$$[MeS] = Me^{2+}_{(initial)} - Me^{2+}_{(residual)} \quad 3.7$$

5 RESULTS AND DISCUSSION

5.1 Effect of Mixing Configuration on Selective Removal of CoS and NiS

The mixing configuration suitable for this study was selected from preliminary work on comparison of selective removal of impurities through a (STR) and a (TPR). The best option was chosen based on the optimal removal of impurities and less co-precipitation with Mn^{2+} ions.

The residual concentrations of Co^{2+}, Ni^{2+} and Mn^{2+} ions that were obtained from both the mixing configurations are presented in Figure 18. The dotted line on each of the graphs, Figure 18 and Figure 19, represents the initial concentration of metal ions on mixing.

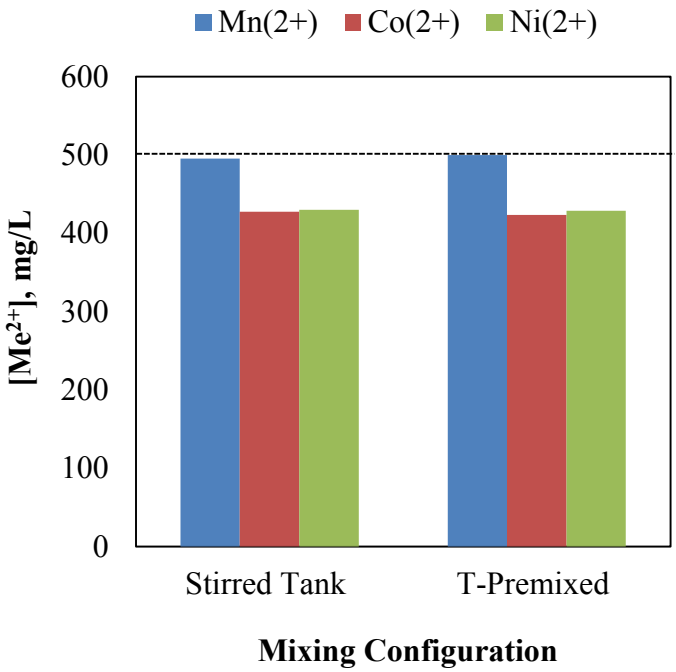

Figure 18: Effect of Mixing Configuration on Removal of CoS and NiS from a Co-Ni-Mn system. Initial concentrations of 580 ppm S^{2-}, 500 ppm Ni^{2+}, 500 ppm Co^{2+} and 500 ppm Mn^{2+}

Immediately one minute after achieving a batch volume of 0.9 L, the data points corresponding to the concentration of Co^{2+}, Ni^{2+} and Mn^{2+} ions in the STR were the same as those in the TPR. An average of 426 ppm of each of the metal ions of Co^{2+} and Ni^{2+} remained in solution, in both the STR and the TPR. That of the Mn^{2+} ions was 500 ppm and 495 ppm

for the TPR and STR respectively. The concentration of the Mn^{2+} did not change of any level of significant from the initial concentration achieved on mixing the two reactants. Therefore, in both cases, the amount of impurities removed and the loss of Mn^{2+} was equally the same, after a batch time of one minute.

On the contrary, Figure 19 shows that on doubling the sulphide concentrations, the average measured residual concentrations of Co^{2+} and Ni^{2+} in a STR was nearly double that in the TPR. The associated loss of Mn^{2+} ions was also higher by 38 ppm compared to that of the TPR. This suggested that the precipitation rate of CoS and NiS was higher for the TPR compared to the STR. This could be due to a micro-mixing time that is faster than that achieved in a STR.

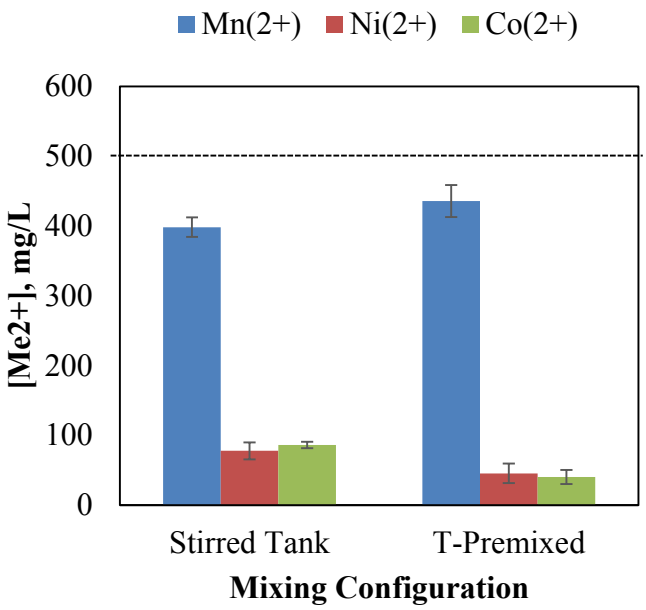

Figure 19: Effect of Mixing Configuration on Removal of CoS and NiS from a Co-Ni-Mn system. Initial concentrations of 1159 ppm S^{2-}, 500 ppm Ni^{2+}, 500 ppm Co^{2+} and 500 ppm Mn^{2+}

A comparison of the data in Figure 18 and Figure 19 showed that the addition of more sulphide ions resulted in a significant increase in the removal of metal ions of Co^{2+}, Ni^{2+} and Mn^{2+} ions from the system. The difference in the removal rates of Co^{2+} and Ni^{2+} for a TPR was approximately 384 ppm per minute for both metal ions. This was relatively higher than the average 347 ppm per minute achieved by the STR. However, the removal of Mn^{2+} was

not that pronounced, the observed difference was 64 ppm and 97 ppm for a TPR and a STR respectively.

This investigation observed that at lower supersaturation (sulphide concentration equal to that of one metal ion) the mixing scale achieved in a STR and TPR are relatively similar. Feeding reactants parallel to each other, at the tip of the impeller exerts a point of high turbulence ensuring better mixing of the two reactants. Similar results were reported in a previous study performed using a semi batch STR (Nienow & Inove 1993).

Increasing the supersaturation level in the system (sulphide concentration equal to that of two metal ions) significantly limited the selectivity of metal ions of Co^{2+} and Ni^{2+} from the electrolyte. In the STR, this difference may be attributed to a creation of different regions of localised supersaturation within the reactor promoting co-precipitation with the Mn^{2+} ions. This is caused by poor dispersion of reactant throughout the reactor volume. This also, may have occurred due to limitations on the impeller speed versus the reactants addition flow rates.

However, for a TPR, the selective removal of Co^{2+} and Ni^{2+} ions was possibly promoted by the difference in the reaction rates for the precipitation of CoS, NiS and MnS. The obtained data suggested that at higher supersaturation levels, the system is mixing limited. The micro-mixing time of 0.002 s used for this investigation was not adequate to match the reaction times necessary for selective precipitation of impurities hence, the co-precipitation with Mn^{2+} ions. It is also important to also acknowledge that these differences may be due to a combination of the equipment, sampling and analytical errors.

5.1.1 Effect of Mixing Configuration on PSD and Morphology

Particle size distribution measurements were taken for both mixing configurations for sulphide concentrations equi-molar to two of the metal ions. Figure 20 shows the percentage volume distribution for the resulting particles from both the STR and the TPR configuration. See Appendix 1B for the raw data obtained from the Malvern Mastersizer.

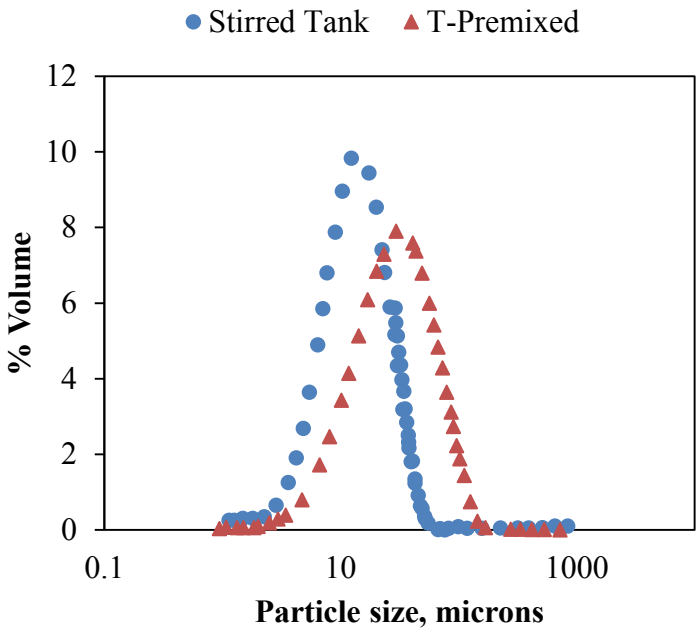

Figure 20: Effect of Mixing Configuration on PSD

The significant percentage volumes of particles were observed for a particle size range 2 -52 µm for a STR and 2-170 µm for that of a TPR. There was a marked difference in the modal particle diameter of the two configurations, on an average of 32.25 µm and 13.97 µm for the TPR and STR respectively. The average $d_{(0.1)}$, $d_{(0.5)}$ and $d_{(0.9)}$ for a TPR were 10.67 µm, 32.25 µm and 76.67 µm and that of the STR was 6.10 µm, 13.97 µm and 29.23 µm respectively. The peak height of the volume distribution obtained for a STR corresponded to a percentage volume of 9.8% for a particles size of 12.4 µm. However that of the TPR was about 1.9% lower and corresponding to a particle size of 29.6 µm. Thus, the STR generated a higher volume of smaller particles compared to the TPR.

The discrepancy between the particle size ranges and the modal particle diameter for the two mixing configurations was possibly due to particle aggregation. Particles between 20 and 100 µm were most likely clumps of smaller particles that adhere to each other through agglomeration. The larger particles in the TPR may also indicate considerable sensitivity to the hydraulic conditions applied promoting particle enlargement due to a domination of aggregation. The precipitation tube used for this investigation had a very small internal diameter of only 0.004 m, thus, the formed particles had a greater probability of colliding with one another within the confined space. Although, it was assumed that there is high turbulence in a TPR, the probability that some reactants did not mix very well is very high.

These would proceed to the receiving vessel, where they create supersaturation and promote growth and aggregation of precipitated particles.

Furthermore, an unexpected narrower particle size distribution resulted from investigations conducted using a STR compared to that of the TPR. However, both of these findings are in contradiction with the results reported by Chiang et al (2007), who observed formation of smaller particles for a TPR compared to those of a STR. This was attributed to the spontaneous nucleation achieved in a TPR compared to a STR. This observation was made for precipitation of a single metal ion stream. Therefore, this contradiction may explain the difference in PSD formed during precipitation from a single metal ion and a multi- metal ionic stream.

It is important to note that all the particles of metal sulphides that were smaller than the filter paper pore size of 0.22 μm were not reported in these PSD as they contributed to the soluble metal fraction (Veeken & Rulkens, 2003; Lewis, Nathoo & Gluck, 2006).

Particles of the precipitates from both mixing configuration were also analysed using SEM, with the objective to identify the morphology of each of the metal sulphides in the mixed precipitate. SEM images were taken for both washed and unwashed precipitates, see Appendix 2B. Images of unwashed precipitates were very poor, they only, distinctly showed the morphology of crystallised ammonium sulphate particles. This was formed when the solvent from the suspension was evaporated with the objective of drying the precipitated particles. Images of washed precipitates showed clustered particles of poor crystallinity. It was also not possible to distinguish the individual sulphides from each other. The XRD analysis confirmed that the particles produced were fine and of amorphous nature. A diffraction pattern of these precipitates could not be produced to ascertain the composition of these precipitates.

5.2 OLI Modelling Results

The expected amount of metal sulphides to be precipitated from a Co-Ni-Mn system of 16000 mg/L Mn^{2+}, 50 mg/L Ni^{2+} ,5 mg/L Co^{2+} and 231 mg/L S^{2-} at varying pH levels of 1 to 10 and temperature of 35 °C, were determined using the OLI Analyser 9.0 software. The

model assumed that the only metal sulphides with ionic products exceeding solubility products precipitate out of the mixed solution at each pH level.

Figure 21 shows the model results on the effect of pH variation on the amount of metal sulphides precipitated. The addition of sulphide ions at pH as low as 1, precipitated about 0.000306 M of NiS. As the operating pH was adjusted to 2, a rapid increase to 0.000816 M of NiS formed was noted. This then gradually increases to reach a maximum of 0.00085 M of NiS between a pH level of 3 and 9. Subsequent increases of pH beyond this point lead to a slight decrease of 0.000017 M of the formed NiS.

Precipitation of CoS also exhibited the same trend; a rapid increase by 0.000082 M of CoS was formed between pH levels of 3 and 5. A further increase in pH by more than one level resulted in the precipitation of the entire CoS in the system. A very rapid decrease in the formation of CoS was noted beyond pH levels of 9. The graph also showed that the trend for the precipitation of MnS is different from that of CoS and NiS. Very small amounts of MnS were initially formed at neutral pH levels. These fluctuate between pH 7 and 9 before significantly increasing to considerable amounts above 0.000001 M.

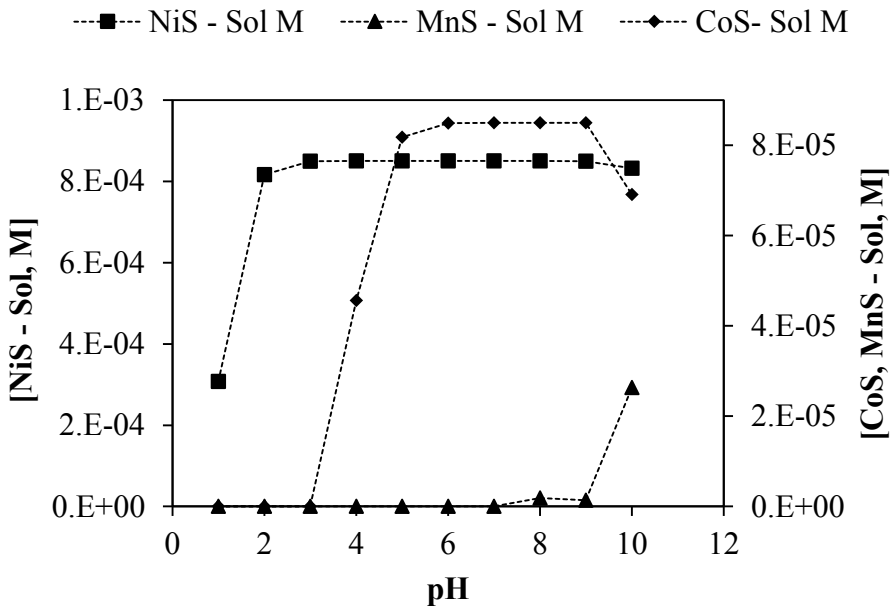

Figure 21: pH dependency of precipitation of CoS, NiS and MnS

Generally, the graph of Figure 21, illustrated that there was an increase in the amount of metal sulphide precipitated with an increase in pH levels. The model illustrated that the

system selectively precipitates NiS only at pH level below 3. Although there was complete precipitation of NiS beyond this pH level, there was also co-precipitation with the CoS. Complete precipitation of both CoS and NiS was only achievable at pH levels between 6 and 9. However, above pH 7, there was a possibility for formation of mixed metal sulphides of Co_x-Ni_y-Mn_z-S_a. Thus, selective precipitation of metal impurities would be ideally controlled at pH level between 6 and 7. Increasing pH beyond this level would also not be a viable strategy for minimizing significant co-precipitation with MnS during the purification process. This may also explain the choice in industrial processes to operate and control pH between 6.8 and 7.2. Purification of this system above pH level of 9 would also be avoided as it significantly favours the precipitation of MnS; this is shown by the tripling in magnitude on the amount of MnS precipitated and reciprocating decrease of NiS and CoS formed. MnS precipitation may be mainly because of the formation of hydroxides of cobalt and nickel, leaving excess sulphide ions to react with Mn^{2+} ions.

The model also confirmed the feasibility to selectively purify the system of Co-Ni-Mn to desired limits below 1 ppm. To test the validity of this model experiments were conducted at pH levels of 4 to 9. At less than pH 4, the speciation of H_2S is limited and may compromise the complete removal of impurities. Four pH levels were chosen and tested, pH 4.8, pH 6.5, pH 7 and pH 7.8. The selection was intended to satisfy the following conditions: pH 4.8 tests complete removal of NiS, pH 6.5 complete removal for both NiS and CoS, pH 7 marks the limit for selective removal of impurities and pH 7.8 tests co-precipitation with MnS.

5.3 Effect of pH on Selective Removal of CoS and NiS

The TPR configuration was adopted to conduct investigations on the effect of pH and batch residence times on selective removal of impurities. The choice of this configuration was based on the fast precipitation rate and optimal selective removal of impurities from a Co-Ni-Mn system. The TPR was also chosen for the additional advantage of promoting the formation of bigger particles of precipitates.

Figure 22 shows the effect of solution pH on the formation of CoS and NiS after a batch time of 45 minutes using a TPR. The standard errors for this data was very small, the error bars could not show on the graph.

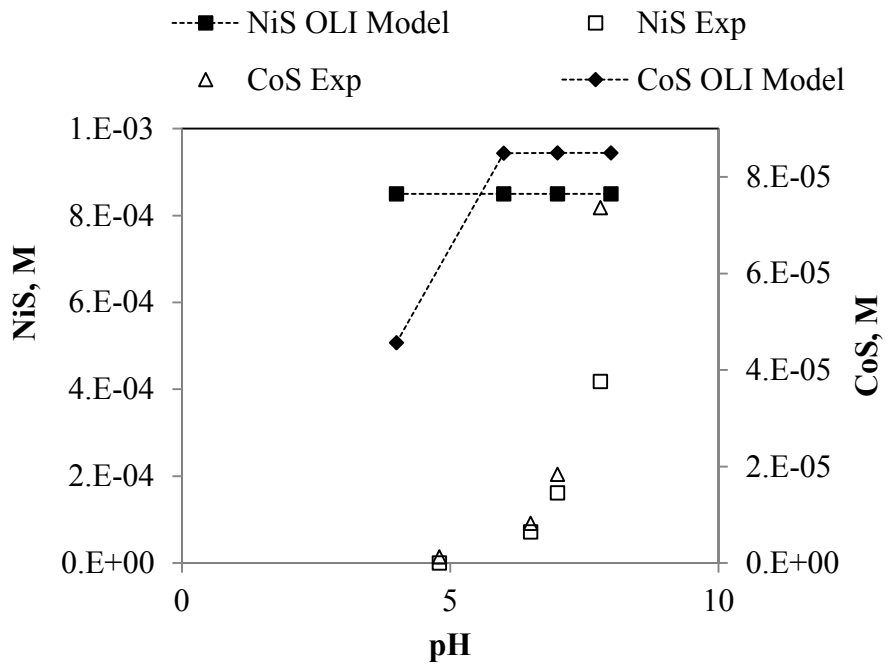

Figure 22: Effect of pH on NiS and CoS precipitation

At pH levels of 4.8, only 0.000013M of CoS precipitated from the system. A further adjustment in the pH level beyond 6.5, promoted simultaneous formation of both CoS and NiS precipitates. The amount of both these precipitates increased significantly on raising pH from 7.0 to 7.8 resulting in the maximum formation 0.0004 M and 0.00007 M of NiS and CoS respectively. The maximum CoS removed was only 49.2% and that of NiS was 86.6 %, at the highest pH investigated.

The corresponding metal sulphide of MnS formed at each pH could not be calculated for this experimental work. An attempt to determine this concentration indicated that the amount of Mn^{2+} ions that was removed from the multi-metal ionic system exceeded the initial amount of sulphide ions available for precipitation. Thus, Mn^{2+} ions were removed from this system by other mechanisms other than the possible formation of MnS.

Therefore, Figure 23 represents the effect of pH on the residual concentration of Mn^{2+} ions. It was observed that this concentration of Mn^{2+} ions decreased considerably between pH 4.8 and 6.5. The point at pH 6.5 corresponding to a residual concentration of 14125 ppm Mn^{2+} ions marked the minimum concentrations recorded for this investigation. A further increase in the pH resulted in a rapid increase in the residual concentration of Mn^{2+} ions. The highest

concentration of 15386 ppm, for this metal ion was recorded at pH of 7.8. Thus, co-precipitation of Mn^{2+} with CoS and NiS decreased with an increase in pH.

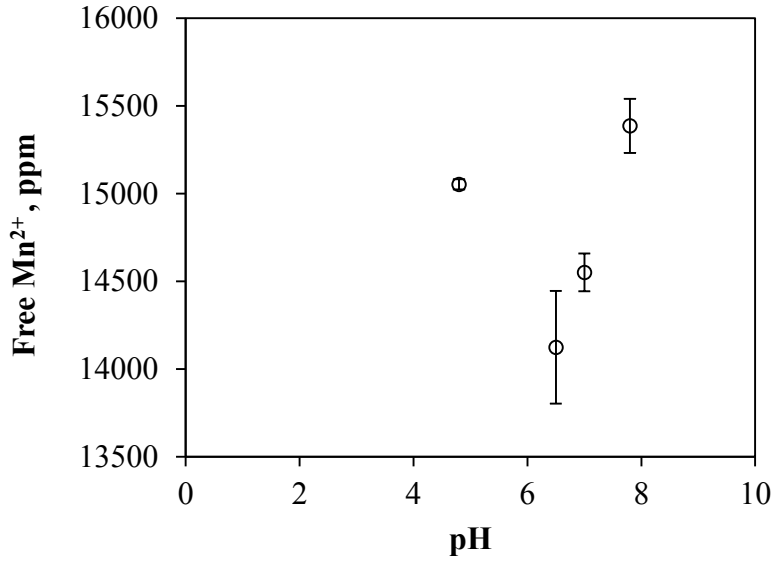

Figure 23: Effect of pH on co-precipitation of Mn^{2+} ions

Interestingly, the percentage loss of these Mn^{2+} ions after 45mins at pH 7.0 is about 9.12%, which is much higher than the 2.63% obtained by Bryson and Bijsterveld (1991). This suggests that the single jet mixing configuration has a less influence on this co-preciptation compared to the TPR configuration. However, the residual concentration of Co^{2+} ions obtained were the same in both experiments.

A comparison on the amounts of impurities and Mn^{2+} ions removed during precipitation, at each pH, suggested that most of the sulphides ions were consumed by the Mn^{2+} ions. The poor formation of NiS and CoS indicated that, at one point, during the precipitation process, there are free sulphide ions present in the system. The influence of local supersaturation possibly promoted instantaneous precipitation of these Mn^{2+} ions. Thus, consuming most of the sulphide ions and limiting the complete precipitation of metal impurities. This precipitation process may have proceeded to form MnS precipitates or metal bisulphides of the form $Mn(HS)_2$ or hydroxides of Mn(OH).SH. This would then limit the amount of sulphide available for precipitating the metal impurities. Assuming Mn^{2+} ions does precipitate to form MnS, this would only constitutes a small percentage of the amount of these ions that is removed from the solution. The fate of the bulk concentration of these metal ions is unknown. Another possible explanation would be attributed to the formation of high order

soluble complex polysulphides of either Co_xS_y or Ni_xS_y or Mn_xS_y instead of the CoS, NiS and MnS assumed in this study (Shea & Helz, 1988; Lewis, Nathoo & Gluck, 2006; Karbanee, van Hille & Lewis, 2008; Mokone, van Hille & Lewis, 2009).

Generally, the effect of pH on formation of CoS and NiS seemed to slightly increase with an increase in pH level. However, the experimentally precipitated amounts were less than those predicted by the OLI thermodynamic model despite the use of an equi-molar concentration of sulphide ions to that of impurities. The trend of this pH effect also, does not follow the thermodynamic pattern, suggesting that the extent of precipitation, at batch times investigated, was influenced by kinetics rather than thermodynamics. Longer batch residence times greater than 45 minutes would be necessary for attempting to fit the model. The desired limits of metal impurities were not achievable at any of the pH levels investigated.

Other observations made during the investigation indicate that the system was able to maintain the pH levels throughout the experiment. There was no need to continuously add a buffer. The different pH levels investigated were achieved by adding a few drops of 0.1 M of sulphuric acid to the mixed metal ion solution.

Immediately after mixing the reactants and during the entire duration of the experiments performed at pH 4.8, the solution remained pink with no visible colour changes or indication of formation of any suspended particles. The collected sample continued to give a pungent smell of hydrogen sulphide suggesting the availability of free sulphide ions for a further reaction. However, the absence of visible suspended particles does not explain the 947 ppm of Mn^{2+} ion calculated to have been removed from the solution. At pH 6.5, few fine black suspended particles of the precipitates were observed under a light source. This observation became more apparent at pH levels of 7.0 and 7.8. However, the amount of particles formed in all three cases was not enough to do further analysis to determine the PSD and composition of the mixed metal sulphide precipitate.

5.4 Effect of batch time on co-precipitation of Mn^{2+} with CoS and NiS

The main objective of this investigation was to identify the mechanism of co-precipitation of Mn^{2+} during selective removal of Co^{2+} and Ni^{2+} ions. Thus, the investigation was conducted at pH level of 7 at maximum limit for this selective removal of impurities.

Figure 24 shows the measure of the residual metal ion concentration of Co^{2+}, Ni^{2+} and Mn^{2+} ions at batch times of 10 min, 30 mins and 45 mins. The concentration of the metal impurities remained virtually constant for the batch times investigated. The concentration of Co^{2+} ions recorded was an average of 3.8 ppm and that of Ni^{2+} ions was 38.8 ppm, 40.8 ppm and 41.5 ppm for the batch times of 10mins, 30mins and 45mins respectively. The slight increase observed on the latter may be related to error associated with sampling, dilution and analysis method used in this study. The concentrations of Co^{2+} and Ni^{2+} achieved were not close to the expected equilibrium concentrations of 0.000001 mg/L and 0.00036 mg/L at this pH level. That of the Mn^{2+} ions increased at an average of 14129 ppm, 14239 ppm and 14540 ppm from 10 mins, 30 mins and 45 mins respectively.

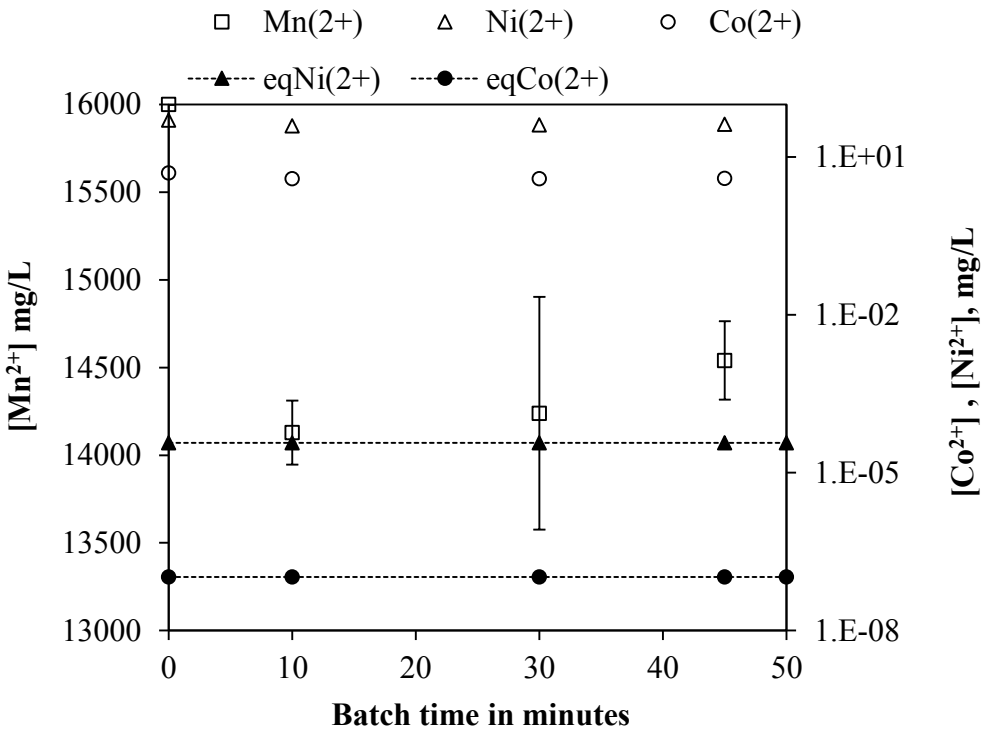

Figure 24: Effect of batch residence time on MnS co-precipitation with CoS and NiS

Assuming that the changes in the concentrations of Ni^{2+} and Mn^{2+} ions suggested dissolution of formed metal sulphides releasing free sulphide ions into solution, the concentration of the Co^{2+} was expected to decrease accordingly. This rules out the possibility for cationic substitution as reported in previous studies for similar systems (McGeorge, Gaylard & Lewis, 2009; Li et al., 2014).

A mass balance on the sulphide ions was difficult to do as the actually amount of these associated with the formation of MnS was unknown. However, the total precipitated metal ions of Co^{2+}, Ni^{2+} and Mn^{2+} exceeded the amount of sulphide ions that were initially available for the reacting with only two impurities of Co^{2+} and Ni^{2+}. This suggests that the bulk of the Mn^{2+} ions are removed from the solution by other mechanisms other than ionic sulphide precipitation. The continuous release of Mn^{2+} ions back into solution would be an indication of a temporary weak physical interaction such as adsorption of ions onto already formed metal sulphides' surfaces. Previous studies suggested that selective sulphide precipitation takes place through both ionic and adsorption processes (Bryson & Bijsterveld, 1991; Veeken & Rulkens, 2003; Lewis, Nathoo & Gluck, 2006). Another logical explanation is the possible formation of complex compounds, with strong bonds of ammonium related ligands, hydroxides or with any other anions is solution.

Due to the fast kinetics of the process, the system was expected to have reached equilibrium at batch time of 10 mins. At shorter batch times than 10 mins, the competitive precipitation of the metal sulphides was expected to be largely influenced by both local supersaturation and reaction kinetics. At longer batch times the difference in solubility products was expected to govern the separation of these metal sulphides. Local supersaturation initially favours the precipitation of Mn^{2+} ions in the bulk solution, whereas the difference in K_{sp} would promote the formation of insoluble CoS and NiS. The latter being more influential as the precipitation approaches equilibrium concentration.

6 CONCLUSIONS AND RECOMMENDATIONS

The main objectives of this study was to understand the effect of pH on selective sulphide removal of Co^{2+} and Ni^{2+} ions from a system of Co-Ni-Mn using a suitable mixing configuration. Furthermore, the research aimed to identify the mechanism of co-precipitation of Mn^{2+} during the purification process.

The following conclusions were drawn from this research work:

- At low supersaturation levels (sulphide concentration equi-molar to one of the metal ion), both the STR and TPR achieved the same selectivity for removal of CoS and NiS. This is due to similar mixing scales in both mixing configurations. Increasing the supersaturation increases the removal rate of impurities through both a STR and a TPR. However, that of the latter is greatest due to faster mixing times achieved by the high reactant flow rate used in this research work.
- The STR produces smaller, fine particles of a narrower PSD compared to those in the TPR. SEM images of the particles formed through TPR indicate that this is possibly due to aggregation which is common with products formed through micro-mixing processes. Industrial application may prefer this method to minimise poor purification due to finer particles. Fine particles of precipitates usually fail to settle, they usually re-dissolve into the bulk electrolyte, increasing the concentration of impurities into the subsequent process.
- Adjusting the pH of a reacting solution does not have a significant effect on the removal of CoS and NiS, to desired residual metal ion concentrations below 1ppm. The concentration of metal impurities remains very high, despite addition of enough sulphide ions to completely remove these impurities. This suggests that sulphide ions are consumed either by the Mn^{2+} ions, or forms complex polysulphides with impurity metal ions or forms strong bonds with other anions in the electrolyte.
- Contrary to thermodynamic predictions, Mn^{2+} ions co-precipitate with CoS and NiS for all the pH levels between 4.8 and 7.8. This decreases with an increase in batch residence time. The possible mechanism of this co-precipitation could not be established due to shorter batch times investigated in this study.
- Few precipitates were produced at 6.5, 7.0 and 7.8 in that order, these were not enough to do PSD, morphology and composition analysis.

The general implication of the above conclusions, on hydrometallurgical systems, is that the purification process is not largely influenced by the operating pH. Further studies are necessary to identify other operating conditions that may significantly reduce the residual concentration of metal impurities to below 1 ppm. These may include seeding and sulphide ion concentration.

Findings also suggest that this process should ideally be conducted at longer batch residence time beyond 45 minutes to minimise loss of Mn^{2+} ions through co-precipitation. However, methods of characterising the solid phase composition of the formed precipitates should be identified to conclusively ascertain the fate of Mn^{2+} ions and confirm complexes of metal sulphides that form during this process. TPR may be preferred for improved production rates and formation of bigger particles, the process may be difficult to monitor and control especially in systems that use pH modifiers.

In conclusion, the influence of local supersaturation on the purification on this purification process may only be understood when the effects of all these aspects are integrated. This is important knowledge for understanding the kinetics of this process for optimisation considerations.

7 REFERENCES

Baldga, J. & Bourne, J.R. 1989. Simplification of micromixing calculations. *Chemical Engineering Journal*. 42:83–92.

Baldyga, J. & Pohorecki, R. 1995. Turbulent micro-mixing in chemical reactors - a review *. *The Chemical Engineering Journal*. 58:183–195.

Benet, N., Muhr, H., Plasan, E. & Rousseax, J.M. 2002. New technologies for precipitation of solid particles with controlled properties. *Powder Technology*. 128:93–98.

Bhagat, M., Burgess, J.E., Antunes, A.P.M., Whitely, C.G. & Duncan, J.R. 2004. Precipitation of mixed metal residues from wastewater utilising biogenic sulphide. *Minerals Engineering*. 17:925–932.

Bhattacharyya, D., Jumawan, A.B., Sun, G., Sund-Hagelberg, C. & Schwitzgebel, K. 1981. Precipitation of heavy metals with sodium sulfide: bench-scale and full-scale experimental results. *In AIChE Symposium Series*. 77(209):31–38.

Bryson, A.W. & Bijsterveld, C.H. 1991. Kinetics of the precipitation of manganese and cobalt sulphides in the purification of a manganese sulphate electrolyte. *Hydrometallurgy*. 27:75–84.

Chiang, Y., Nathoo, J. & Lewis, A.E. 2007. Investigating the control of manganese sulphide precipitation. *Southern African Institute of Mining and Metallurgy*. 107:231–236.

Cibati, A., Cheng, K.Y., Morris, C., Ginige, M.P., Sahinkaya, E., Pagnanelli, F. & Kaksonen, A.H. 2013. Selective precipitation of metals from synthetic spent refinery catalyst leach liquor with biogenic H2S produced in a lactate-fed anaerobic baffled reactor. *Hydrometallurgy*. 139:154–161.

Gharabaghi, M., Irannajad, M. & Azadmehr, A.R. 2012. Selective sulphide precipitation of heavy metals from acidic polymetallic aqueous solution by thioacetamide. *Industrial & Engineering Chemistry Research*. 51(2):954–963.

Gradl, J. & Peukert, W. 2010. Characterisation of micromixing for precipitation of nanoparticles in a T-mixer. In *Micro and Macro-mixing*. Springer Berlin Heidelberg. 105–124.

Grulietti, M., Seckler, M.., Derenzo, S.R. & Cekinski, E. 2001. Industrial crystallisation and precipitation from solution: State of the technique. *Brazilian Journal of Chemical Engineering*. 18(4):423.

Harris, M., Meyer, D.M. & Auerswald, K. 1977. The production of electrolytic manganese in South Africa. *Southern African Institute of Mining and Metallurgy*. 77(7):137–142.

Jackson, E. 1986. *Hydrometallurgical Extraction and Reclamation*. G. West E & OBE, Eds. West Sussex: Ellis Horwood Limited.

Jacobs, J.H. 1946. Effects of cell variables on the electrowinning of manganese. In *Ninetieth General Meeting*. 211–220.

Jandová, J., Lisá, K., Vu, H. & Vranka, F. 2005. Separation of copper and cobalt–nickel sulphide concentrates during processing of manganese deep ocean nodules. *Hydrometallurgy*. 77:75–79.

Jha, C.M., Wicker, R.G. & Meyer, A.G. 1978. *Patent No. 820595*. United States Patents.

Kamal, S., Mazlina, Z.M., Nik, N.A. & Abdul-talib, S. 2011. Removal of nickel through biological sulphide precipitation. *Research Journal of Chemistry and Environment*. 15(2):359–364.

Karbanee, N., van Hille, R.P. & Lewis, A.E. 2008. Controlled nickel sulfide precipitation using gaseous hydrogen sulfide. *Industrial and Engineering Chemistry Research*. 47(5):1596–1602..

Kolthoff, I.M. & Moltzau, D.R. 1935. Induced precipitation and properties of metal sulfides. *Chemical Reviews*. 17(3):293–325.

Kugler, R., Doyle, S. & Kind, M. 2014. Precipitation kinetics of barium sulfate at high supersaturation by in-situ synchrotron radiation WAXS. In *19th Internatiional Symposium on Industrial Crystallization*. 100–102.

Lewis, A.E. 2010. Hydrometallurgy review of metal sulphide precipitation. *Hydrometallurgy*. 104(2):222–234.

Lewis, A.E. & van Hille, R.P. 2006. An exploration into the sulphide precipitation method and its effect on metal sulphide removal. *Hydrometallurgy*. 81(3-4):197–204.

Lewis, A.E. & Swartbooi, A. 2006. Factors affecting metal removal in mixed sulfide precipitation. *Chemical Engineering & Technology*. 29(2):277–280.

Lewis, A., Seckler, M., Kramer, H. & van Rosmalen, G. 2012. *Industrial crystallisation in practice, from basics to applications*. 1st ed. Campbridge University Press (prep).

Lewis, A.E., Nathoo, J. & Gluck, T. 2006. Identifying critical operatin parameters and mechanism for manganese sulphide precipitation process. In *Bremen International Workshop on Industrial Crystallisation*. 1–8.

Li, L., Chen, X., Liu, X. & Zhao, Z. 2014. Removal of Cu from the nickel electrolysis anolyte using amorphous MnS. *Hydrometallurgy*. 146:149–153.

Luther, G.W. & Rickard, D.. 2005. Metal sulphides cluster complexes and their biogeochemical importance in the environment. *Journal of Nanoparticles*. 7:389–407.

McGeorge, B., Gaylard, P.G. & Lewis, A.E. 2009. Mechanism of rhodium(III) co-precipitation with copper sulfide (at low Rh concentrations) incorporating a new cationic substitution reaction path. *Hydrometallurgy*. 96(3):235–245.

Mersmann, A. 2001. *Fundamentals of Crystallisation*. M. Dekker, Ed. New York.

Mishra, P.K. & Das, R.P. 1992. Kinetics of zinc and cobalt sulphide precipitation and its application in hydrometallurgical separation.pdf. *Hydrometallurgy*. 28(3):373–379.

Mokmeli, M., Wassink, B. & Dreisinger, D. 2013. Kinetics study of selenium removal from copper sulfate–sulfuric acid solution. *Hydrometallurgy*. 139:13–25.

Mokone, T.P., van Hille, R.P. & Lewis, A.. 2009. Mechanisms responsible for particle formation during metal sulphide precipitation processes. In *International Mine Water Conference*. Pretoria: Document Transformation Technologies. 343–350.

Mullin, J.W. 2001. *Crystallisation*. Fourth Edi ed. Oxford: Butterworth-Heinemann.

Myerson, A.. 2002. *Handbook of Industrial Crystallisation*. 2nd ed. Boston,USA: Butterworth Heinemann Ltd.

Ntuli, F. & Lewis, A.E. 2009. Kinetic modelling of nickel powder by high pressure hydrogen reduction. *Chemical Engineering Science*. 9(64):2202–2215.

O' Grady, D. 2011. *Supersaturation: Driving force for nucleation and growth. Online Mettler Toledo*. Available: http//blog.autochem.mt.com/2011/03/supersaturation-driving-force-for-crystallisation-nucleation-growth/

Peters, R.W., Young, K. & Bhattacharyya, D. 1985. Evaluation of recent treatment techniques for removal of heavy metals from industrial wastewater. *AICHE Symposium Series*. 81(243):165–203.

Randolph, A.D. & Larson, M.A. 1988. *Theory of Particulate Processes: Analysis and Techniques of Continuous Crystallisation*. 2nd ed. San Diego, California: Academic Press.

Reis, F.D., Silva, A.M., Cunha, E.C. & Leão, V.A. 2013. Application of sodium and biogenic sulfide to the precipitation of nickel in a continuous reactor. *Separation and Purification Technology*. 120:346–353.

Rice, R.W. & Baud, R.E. 1990. The role of micromixing in the scale up of geometrically similar batch reactors. *AICHE*. 36:293–298.

Rickard, D. 1989. An apparatus for the study of fast precipitation reactions. *Mineralogical Magazine,*. 53(December):527–530.

Roelands, B.M., Derksen, J., Horst, J., Kramer, H. & Jansens, P. 2003. An analysis of mixing in a typical experimental setup to measure nucleation rates of precipitation processes. *Chemical Engineering & Technology*. 26(3):296–302.

Sahinkaya E., Gungor M., Bagrakdar A., Yucesoy Z. & Uyanik S. 2009. Separate recovery of copper and zinc from acid mine drainage using biogenic sulphides. *Journal of hazardous Materials*. 171(1-3):9001–906.

Sampaio, R.M.M., Timmers, R.A., Xu, Y., Keesman, K, J. & Lens, P.N.L. 2009. Selective precipitation of Cu from Zn in a pS controlled continuously stirred tank reactor. *Journal of hazardous materials*. 165:256–265.

Shea, D. & Helz, G.R. 1988. The solubility of copper in sulfidic waters: Sulphides and polysulphides in equilibrium with covellite. *Geochimica et Cosmochimica Acta*. 52:1815–1825.

Siame, J. & Kasaini, H. 2013. Selective precipitation of Pt and base metals in liquid-liquid chloride systems. In *International Conference on Chemical and Environmental Engineering*. Johannesburg. 88–95.

Sohnel, O. & Garside, J. 1992. *Precipitation,Basic Principles and Industrial Applications*. Manchester: Butterworth Heinemann Ltd.

Stumm, W. & Morgan, J.J. 1996. *Aquatic Chemistry:Chemical Equilibria and Rates in Natural Waters*. 3rd ed. New York: John Wiley and Sons.

Torbacke, M. & Rasmuson, A.. 2001. Influence of different scales of mixing in reactive crystallisation. *Chemical Engineering Science*. 56:2459–2473.

Veeken, A.H.M. & Rulkens, W.H. 2003. Innovative developments in the selective removal and reuse of heavy metals from wastewaters. *Water Science and Technology*. 9–16.

Vicum, L., Ottiger, S., Mazzotti, M., Maskowski, L. & Baldyga, J. 2004. Multi-scale modelling of reactive mixing processes in a semi batch stirred tank reactor. *Chemical Engineering Science*. 59:1767–1781.

Villa-Gomez, D.K., Papirio, S., van Hullebusch, E.D., Farges, F., Nikitenko, S., Kramer, H. & Lens, P.N.L. 2012. Influence of sulfide concentration and macronutrients on the characteristics of metal precipitates relevant to metal recovery in bioreactors. *Bioresource Technology*. 110:26–34.

Wanamaker, E.M. & Morgan, W.D. 1943. *Patent No. 2,325,123*. United States.

Wu, C.C. & Yang, M.H. 1976. The retention behaviour of radionuclides on copper(II) sulphide. *Analytica Chimina Acta*. 84(2):335–345.

8 APPENDICES

APPENDIX A - Design Specifications of T-premixed reactor (TPR)

1. d< D where d is inner diameter and D is the outer diameter

Inner diameter of outlet pipe should be significantly smaller than injector inner diameter.(Rice & Baud, 1990)

Injector Outer Diameter 6.0mm

Injector Inner Diameter 4.0mm

2. Inlet tube length (L)

L/D should be greater than 10 for fully developed turbulent flows.

Thus length of inlet pipes should be 4mm X 20 = 80mm

3. Calculating Average flow velocity, U

$$U = \frac{Total\ flow\ rate}{Area}$$

$$U = \frac{4\,Q}{\pi D^2}$$

The combined maximum output for the two magnetic drive gear pumps is 20ml/s.

Therefore:

$$U = \frac{4\ x\ 0.000020 m^3/s}{\pi(0.004m)^2}$$

$$U = 1.59 m/s$$

4. Calculating Reynolds Number

Lamina flow: Re < 2300

Transition flow: 2300 < Re < 4000

Turbulent flow Re > 4000

$$Reynold\ Number = \frac{UD}{v}$$

Where: U = average flow velocity, ms^{-1}

D = hydraulic diameter, m

v = kinematic viscosity, m^2s^{-1} Q = flow rate, m^3/s

$$Re = \frac{1.59m/s\ (0.004m)}{10^{-6}m^2s^{-1}}$$

$$Re = 6369.4$$

5. Calculating the mean dissipated rate:

$$\varepsilon = \frac{Q\Delta P}{\rho V} = \frac{2fU^3}{D}$$

$$f = 0.316\ \mathrm{Re}^{-0.25}$$

The Blasius equation is the most simple equation for solving the Darcy friction factor. Blasius equation is valid only to smooth pipes. The Blasius equation is valid up to the Reynolds number 10^5 .

$$\varepsilon = 71.409 m^2 s^{-3}$$

6. Calculating the micro-mixing time:

The Kolmogorov's turbulence theory of smallest eddies suggest the micro-mixing time can be calculated as:

$$\tau = 17.24\sqrt{(v/\varepsilon)} \qquad \textit{(J.Baldga \& J.R.Bourne)}$$

$$\tau = 0.0020s$$

APPENDIX 1B – Mastersizer Particle Size Distribution Data

Table 3: Percentage volume distribution for particle sizes in a TPR

Size µm	Run 1 % Volume	Run 2 % Volume
1.0 - 2.0	0.00	0.00
2.0 - 3.0	0.20	0.12
3.0 - 5.0	1.21	0.96
5.0 - 7.0	2.27	1.52
7.0 - 10.0	4.89	2.64
10.0 - 13.0	5.79	2.67
13.0 - 19.0	12.06	5.67
25.0 - 38.0	11.37	6.93
38.0 - 53.0	20.57	18.69
53.0 - 75.0	16.76	21.34
75.0 - 106.0	14.17	21.81
106.0 - 150.0	8.04	13.59
150.0 - 212.0	2.52	4.05

Table 4: Percentage volume distribution for particle sizes from a STR

Size µm	Run 1 % Volume	Run 2 % Volume
1.0 - 2.0	0.92	.
2.0 - 3.0	0.69	97
3.0 - 5.0	3.52	0.86
5.0 - 7.0	7.71	4.05
7.0 - 10.0	15.92	7.99
10.0 - 13.0	16.26	15.67
13.0 - 19.0	25.03	15.67
25.0 - 38.0	14.66	24.09
38.0 - 53.0	12.31	14.41
53.0 - 75.0	2.68	12.77
75.0 - 106.0	0.17	3.12
106.0 - 150.0	0.00	0.23
150.0 - 212.0	0.00	0

APPENDIX 2B – SEM Images

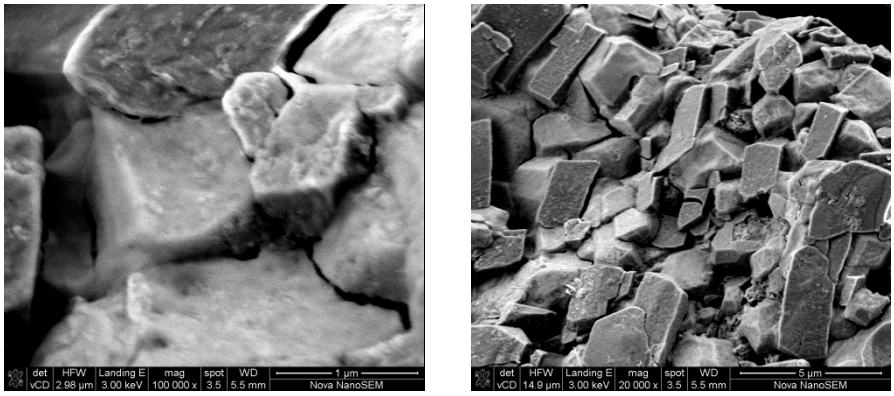

Figure 25: SEM images of unwashed metal sulphide precipitates

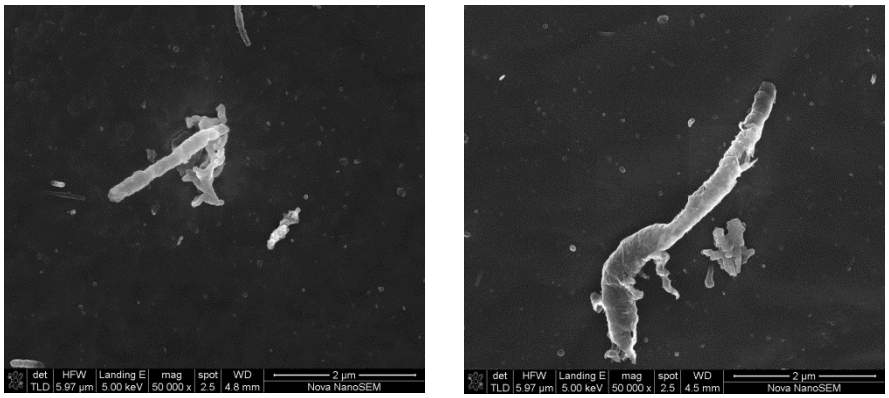

Figure 26: SEM images of washed mixed metal sulphides from a STR and TPR configuration respectively

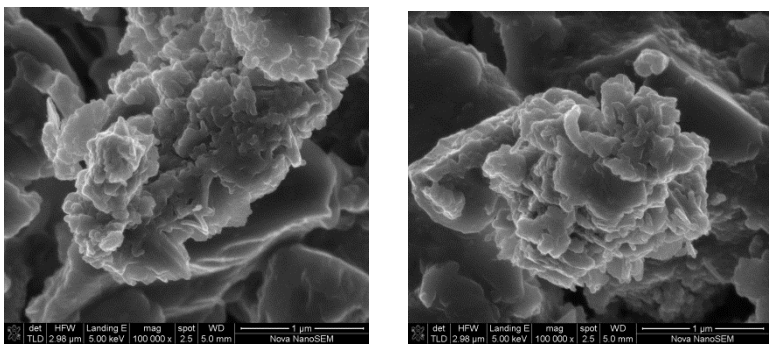

Figure 27: SEM images for washed mixed metal sulphides

APPENDIX C – Calculation of Precipitated Metal Sulphides

Residual Metal Ion Concentrations

The concentration of metal ions that remained after precipitating the metal sulphides was determined using the ICP-OES analysis. The results are given below:

Table 5: Residual Metal Ion Concentrations as obtained from ICP-OES analysis for Run 1A 1B and 1C

Run 1A	**Co^{2+}**	**Ni^{2+}**	**Mn^{2+}**
pH	**(ppm)**	**(ppm)**	**(ppm)**
4.8	4.98	49.88	15136.00
6.5	4.76	47.79	15034.00
7.0	3.78	40.87	14857.00
7.8	0.67	24.84	14950.00
Run 1B	**Co^{2+}**	**Ni^{2+}**	**Mn^{2+}**
pH	**(ppm)**	**(ppm)**	**(ppm)**
4.8	4.89	49.60	14971.00
6.5	4.29	43.62	13216.00
7.0	4.08	39.96	14246.00
7.8	0.67	25.86	15823.00
Run 1C	**Co^{2+}**	**Ni^{2+}**	**Mn^{2+}**
pH	**(ppm)**	**(ppm)**	**(ppm)**
4.8	4.94	49.74	15053.50
6.5	4.53	45.71	14125.00
7.0	3.93	40.42	14551.50
7.8	0.67	25.35	15386.50

Metal Sulphides Calculations

The precipitated metal sulphides were calculated using Equation 3.7 in Section 4.7. The molar masses of Co^{2+} ,Ni^{2+} and Mn^{2+} used for the conversion of ICP-OES concentrations from ppm to molarity were 58.93 g/mol, 58.70g/mol and 54.93 g/mol respectively. The MnS calculated is related to the concentration of metal ions that is not in solution. This was done to compare this value to the sulphide ion concentration, initially available for precipitation.

Table 6: Calculated Metal sulphides formed at each pH level for Run 1A, 1B and 1C

Run 1A	**CoS**	**MnS**	**NiS**
pH - Aqueous	**M**	**M**	**M**
4.8	5.0.E-07	1.6.E-02	2.9.E-07
6.5	4.2.E-06	1.8.E-02	3.6.E-05
7.0	2.1.E-05	2.1.E-02	1.5.E-04
7.8	7.4.E-05	1.9.E-02	4.3.E-04

Run 1B	**CoS**	**MnS**	**NiS**
pH - Aqueous	**M**	**M**	**M**
4.8	2.0.E-06	1.9.E-02	5.0.E-06
6.5	1.2.E-05	5.1.E-02	1.1.E-04
7.0	1.6.E-05	3.2.E-02	1.7.E-04
7.8	7.4.E-05	3.2.E-03	4.1.E-04

Run 1C	**CoS**	**MnS**	**NiS**
pH - Aqueous	**M**	**M**	**M**
4.8	1.3.E-06	1.7.E-02	2.7.E-06
6.5	8.2.E-06	3.4.E-02	7.1.E-05
7.0	1.8.E-05	2.6.E-02	1.6.E-04
7.8	7.4.E-05	1.1.E-02	4.2.E-04